RECENT PROGRESS AND CHALLENGES IN HEAT PIPES SCIENCE

Lips S.*
*Author for correspondence
CETHIL UMR5008, Center for Energetics and Thermal Sciences of Lyon,
University of Lyon, CNRS, INSA-Lyon,
69621 Villeurbanne cedex,
France,
E-mail: stephane.lips@insa-lyon.fr

ABSTRACT

Despite the numerous studies on heat pipes for fifty years, the development of predictive tools for the design of heat pipes is still challenging, even for conventional technologies. It results in a real limitation in the spread of heat pipes in the industry as each new heat pipe has to be carefully designed for a specific application. The present communication aims at identifying and understanding the current scientific problems of heat pipe science. The different types of heat pipe are reviewed in order to identify the main phenomena involved in these systems. A global review of the recent studies on heat pipes is then presented. Advances are identified in the fields of the heat pipe characterization, on the working fluid problematic, on the understanding of phase change heat transfer in thin liquid films and on the system modeling. Two examples of recent works are also detailed to highlight the strategies that can be followed to answer the current issues. This global review enables to highlight the main advances on heat pipe science of these last five years and to draw perspectives on the forthcoming science progresses.

INTRODUCTION

Heat pipes are widely used in many industrial applications. They enable the transfer of high heat fluxes with low temperature gradients by using the latent heat of vaporization of a working fluid. The diversity of the different kinds of heat pipes is an image of the diversity of the conditions in which they are used. However, whatever the type of heat pipe, their normal behaviour is bounded by several working limits that depend on various phenomena. They are the object of thousands of scientific articles published in dozens of international journals. Two international conferences are dedicated to them every fourth year and they are present at all general conferences dedicated to heat transfer. For instance, 11 communications dealt with heat pipes in HEFAT 2014. However, despite the numerous studies on heat pipes for fifty years, the development of predictive tools for the design of heat pipes is still challenging, even for conventional technologies. It results in a real limitation in the spread of heat pipes in the industry, as each new heat pipe has to be carefully designed for a specific application. By a means of a review of the recent works published on heat pipe, the present communication aims at understanding the scientific key issues that lead to this situation and the strategies that can be used to progress towards a better understanding of the different types of heat pipes.

In a first part, the different types of heat pipe are reviewed in order to identify the main phenomena involved in these systems. In a second part, a general study is realized based on the titles of the articles published on heat pipes. The recent advances are then detailed and classified in terms of system characterization, fluid behaviour problematic, phase change heat transfer in thin films and heat pipe modelling. Two examples of recent results are detailed in order to highlight possible strategies for answering some of the encountered issues. Conclusions and perspectives are finally drawn.

OVERVIEW OF HEAT PIPE TECHNOLOGIES

A heat pipe is a system able to transfer high heat fluxes with a low thermal resistance using liquid-vapour phase change [1]. They consist of a cavity filled by a fluid at saturation. The liquid evaporates at the contact of a heat source and condensates close to a heat sink. The way the vapour and the liquid flow to the condenser and to the evaporator respectively depends on the type of heat pipe. The main types of heat pipes are summarized in figure 1. The distinction can be made between conventional heat pipes, loop heat pipes and oscillating heat pipes.

Conventional heat pipes regroup thermosyphons, cylindrical heat pipes, flat plate heat pipes and rotating heat pipes. The liquid and vapour flows are countercurrent within the heat pipe body. The liquid flows form the condenser to the evaporator thanks to either gravity, capillary or centrifugal forces. In capillary heat pipes, the capillary structure (grooves, meshes or porous medium) has to be continuous from the condenser to the evaporator.

The term loop heat pipes regroups loop heat pipes themselves (LHP), but also capillary pumped loops (CPL) and two-phase loop thermosyphons. The liquid and vapour flow in separate lines and the sum of frictional and gravitational pressure drops are compensated by the capillary forces in the capillary structure placed at the evaporator only. A CPL differs from a LHP by the place of the reservoir, which has a great importance on the system behaviour.

The oscillating heat pipes, also called pulsating heat pipes (PHP) are made of a single meandering tube place between the heat source and the heat sink. Its diameter close to the fluid capillary length leads to a liquid plug and vapour slug

distribution within the tube. In the evaporator, the violent vaporization of the liquid slug generates self-sustained oscillations of the fluid, which lead to an efficient heat transfer from the heat source to the heat sink, both by latent and sensible heat. These systems are cheap and easy to manufacture, but their behaviour is difficult to predict and there are sparsely used in the industry.

Despites the strong differences between the different heat pipe technologies, there are several phenomena shared by these systems. Obviously, liquid-vapor phase change heat transfer is present in all heat pipes. The phase change occurs at the scale of the capillary structure or at the scale of the thin liquid films present in the system. The capillary forces are indeed almost never negligible. Moreover, as the fluid is always heated through a wall, the interactions between the working fluid and the wall are of great importance. Lastly, there is always a coupling between hydrodynamic and thermal phenomena as the working fluid follows a thermodynamic cycle in the systems.

To summarize, the induced scientific issues can generally be classified in four types:

- The understanding of the behaviour of the working fluid in a capillary structure and the prediction of the resulting properties of the capillary structure filled with the working fluid.
- The prediction of heat transfer in thin liquid films during evaporation or condensation.
- The prediction of the system behaviour due to the coupling of the different phenomena.
- The understanding of the physicochemical interaction between the working fluid and the other heat pipe materials.

In the remaining of the document, works on heat pipes are classified according to type of studies and not to the type of systems. The similarity of the phenomena involved in all heat pipes induces that the progress in understanding of one kind of heat pipes generally help progress on the others kinds.

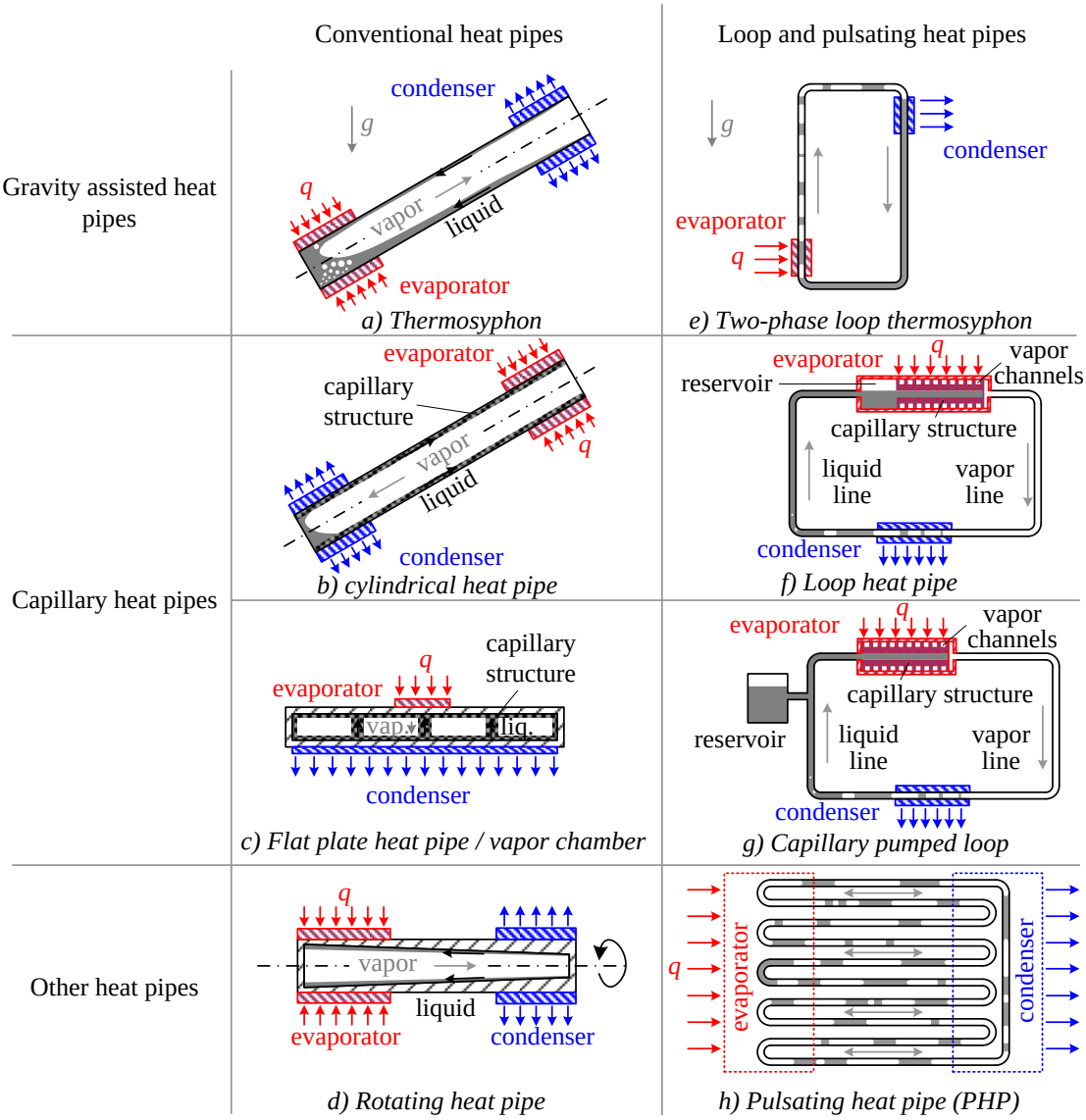

Figure 1 Different heat pipe technologies

CURRENT RESEARCH IN HEAT PIPE SCIENCE

In order to have an overview of the current research in heat pipe science, a global analysis of the studies published on heat pipe is realised. Figure 2 presents the evolution of the number of paper related to heat pipes indexed on the Web Of Science™ database between 1975 and 2014. Table 1 summarizes the exact query used to plot the figure 2. Several technologies are distinguished by filtering the content on the article title only, so the present analysis does not pretend to be exhaustive, but rather aims at giving the general trends of research in heat pipes during the last forty years. The heat pipe science began during the sixties and conventional heat pipes were soon widely used in space applications. During the eighties, terrestrial applications of heat pipes are developed, mainly with thermosyphons because of the difficulty overcoming the gravity forces. During the nineties, new types of heat pipes are invented and more and more studied. Micro heat pipe appears thanks to the progress of micro technologies and the progresses in porous technologies enable the development of CPL and LHP.

Since 2000, the number of paper dedicated to heat pipes increases continuously and reaches now about 250 papers per year. This great number of research is mainly motivated by the increase of the power of electronics components, which creates a need in efficient and reliable cooling systems. Heat pipes are thus developed for terrestrial applications and the systems need to be optimized and perfectly understood in order to deals with gravity forces. In the same time, the increase of the energy price promotes the use of heat pipes in numerous applications, either as a passive system to evacuate heat or to improve the efficiency of heat recovery systems. In parallel, the continuous progress in new materials and manufacturing processes carry the spread of heat pipes in industrial applications.

Table 1 Queries corresponding to Figure 2

Type of heat pipe	Query (in title)	Total results
All kind of heat pipes	"heat pipe(s)" or thermosyphon(s) or thermosiphon(s) or "vapo(u)r chamber(s)" or "capillary pumped loop(s)"	3634
Thermosyphon*	thermosyphon(s) or thermosiphon(s)	820
Rotating heat pipe	rotating and "heat pipe(s)"	49
Micro heat pipe	"micro heat pipe(s)"	112
Flat heat pipe	"Flat (plate) heat pipe(s)"	119
LHP	"loop heat pipe(s)"	325
CPL	"capillary pumped loop(s)"	75
PHP	(pulsating or oscillating) and "heat pipe(s)"	334
Vapour chambers	"vapo(u)r chamber(s)"	117

*the term thermosyphon can also refers to single-phase thermosyphons. A global analysis of the abstracts shows that they represent between 15 and 20 % of the papers mentioning the term "thermosyphons" in their title.

In figure 2, one can note the important development of research on LHP for 15 years and on PHP for 10 years. Together, they represent currently almost half of the paper devoted to heat pipe. One can also note the remaining importance of research on thermosyphons, despite the age of the early research on this field. The category "others" in figure 2 refers to all papers for which the type of heat pipe has not been identified through the title. They often refer to conventional cylindrical heat pipes, but also to study dedicated to phenomena involved in heat pipe in general.

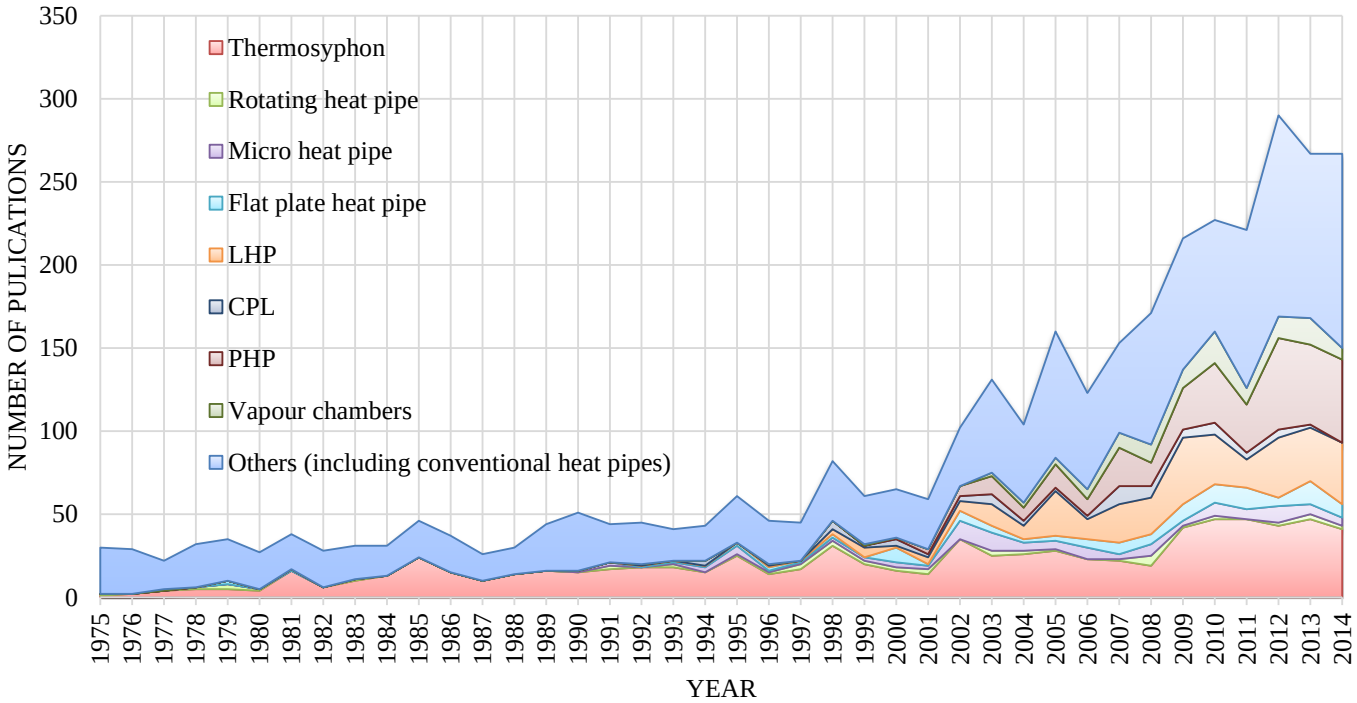

Figure 2 Evolution of the number of papers dedicated to heat pipes according to the database of Web Of Science™

In 2007, Riffat and Ma [2] proposed a review of developments in heat pipe technology and applications between 2000 and 2005. They noted different kinds of advance during the period. New kinds of wick structure for conventional and flat heat pipes were proposed as well as new working fluids. They highlighted the development of new types of loop heat pipes (LHP and CPL) that were expected to be widely used in industrial application. They also noted studies on flexible heat pipes as well as on micro heat pipes. New applications were studied as solar collector systems and heat pipe turbines. Traditional topics as high temperature heat pipe and space applications were also reported. For air conditioning system, the coupling between phase change material and heat pipes were investigated. Lastly, they reported the development of new models and mathematical methods for the design of different kinds of heat pipes.

Ten years later, the research field on heat pipes changed strongly. Figure 3 presents a word cloud realized from the titles of the articles published on heat pipes between 2012 and 2014 (about 800 papers). In this word cloud, the size of the words is proportional to the square root of the number of occurrence of each words. It is a convenient tool to have a general overview of a given field. Besides the words directly related to the heat pipes themselves and their main components, it appears that *experimental* works are dominant compared to *simulations*, *numerical* analyses and *modeling*. On the other side, *Analytical* approaches are very rare. Papers often interest in heat pipe *performance* and the diversity of the applications appears, even in the paper titles (*electronic cooling*, *LED*, *air conditioning*, *solar collector*, *cryogenic* applications, *vehicles*, *thermoelectric generators, energy storage*…). One can note the importance of the working fluid (*water*, *ethanol*, *mixture*) and materials (*metal*, *copper*, *silicon*, *aluminium*, *glass*, *ceramic*, copper oxide (*CUO*)) used in heat pipes, as they explicitly appear in many paper titles. The link between heat pipe science and material science is highlighted by the important occurrence of the words *nanofluid(s)* and *carbon nanotubes*. Progress in manufacturing also promotes the development of *micro* heat pipes as well as of *light weigh* heat pipes.

This word cloud also gives a brief summary of the subject of the studies; effect of *gravity* forces and *inclination* angles are studied, as well as *magnetic* and *electric* fields. The *start-up* procedure is the topic of several articles and their *transient response* is studied. The word cloud even gives clues on some experimental devices used to characterize heat pipes, as *neutron radiography*.

If the word cloud enables to highlight the main keywords describing the current research on heat pipe, it does not give information on the content of the articles. The present keynote aims at summarizing the main advances on heat pipes published in the recent studies. In the remainder of the article, the different scientific questions are classified in four categories:

- Heat pipe characterisation (at the scale of the system or of the different components).
- Fluid behaviour problematic.
- Phase change heat transfer in thin films.
- System modelling.

Figure 3 Word cloud corresponding to the titles of the papers on heat pipes published between 2012 and 2014 (200 top used words of about 800 papers)

SYSTEM CHARACTERIZATION

Heat pipe performance determination

For an industrial point of view, an important outcome of heat pipe studies is the determination of the global performance of the different heat pipes. The performance can be expressed in terms of system thermal resistance and of system capacity to work in given operating conditions (imposed heat flux, ambient temperature, acceleration, orientation…). Many studies are thus devoted to the determination of the heat pipe performance and the numerous prototypes that are tested enable to build important database for each type of heat pipes. As an example, Maydanik *et al*. [3] proposed recently a review on the performance of loop heat pipes with flat evaporators. The performance of the different geometries are compared, as well as the impact of the working fluid and the materials. Recommendations are then proposed in order to achieve a good performance when designing the evaporator of a LHP.

Besides academic papers, many patents are deposited, in which specific geometries and configurations are proposed. Patents can deal with specific parts of heat pipe, as condensers [4] or wicks [5]. Additional parts are also proposed, as a reservoir filled with adsorbent material in order to deal with freezing problems [6].

In a general way, each time a new heat pipe design is proposed, the first step in studying a prototype is to determine his performance. As an example, Lachassagne *et al*. proposed a new kind of LHP, called CPLIP, with a reservoir placed located the evaporator. In a first paper they determined its performance [7], and then proposed a model in steady state conditions [8].

Capillary structure characterization

The development of models for capillary heat pipe requires the knowledge of the properties of their capillary structure filled with the working fluids as they have a direct effect on the heat pipe performance.

Consequently, the capillary structures are the object of great attention in heat pipe sciences. New way of manufacturing new capillary structure are developed continuously. For instance, Singh *et al.* presented their fabrication technique for a sintered aluminum evaporator of a Loop heat pipe [9]. Santos *et al.* proposed on their side an evaporator made of ceramic [10]. Their experience helps develop evaporators that are still more advanced in the future.

Besides developing new capillary structures with new techniques and new materials, a strong challenge is to determine the properties of existing capillary structures and to develop predictive tools that can be used in heat pipe models. The measure of the capillary structure permeability can be performed easily [11,12] but the determination of its equivalent thermal conductivity is more difficult. It can be performed with a flash method for instance [13] but the measured value take into account only conduction through the capillary structure and does not consider evaporation or condensation phenomena. More sophisticated set-ups has to be developed to take into account these phenomena [14].

Example of contribution of inverse method

When direct measurements cannot be performed, another approach consists in using inverse methods. This approach is illustrated in this section with a novel method proposed by Revil-Baudard and Lips [15]. It aims at determining the capillary structure properties from flat plate heat pipe global performance measurements for different inclination angles. The determination of the thermal properties is based on an analytical method that is directly inverted: the equivalent thermal conductivity of the capillary structure at the condenser and at the evaporator are thus the outputs of the inverse method, whereas the temperature measurements along the heat pipe are the inputs (figure 4). This simple and powerful technique enables a direct comparison between the capillary structure properties of different heat pipes even if the global thermal resistance of the systems are different. It is the first step for the construction of an experimental equivalent thermal conductivity database for the development of predictive tools.

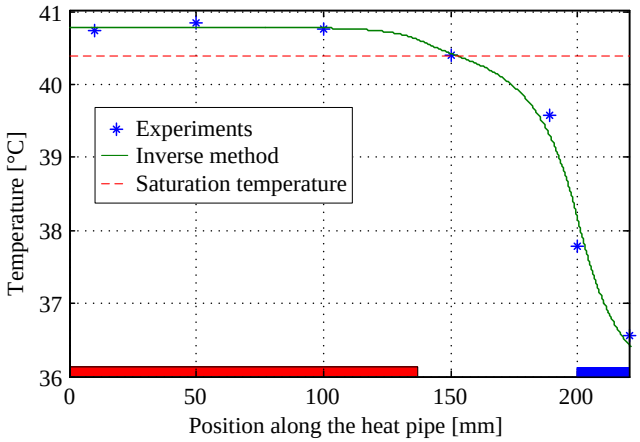

Figure 4 Example of comparison between an experimental temperature profile and the corresponding profile calculated by the inverse method for a FPHP [15]

The determination of the hydrodynamic properties of the capillary structure, i.e. its permeability and its effective pore radius is more difficult as no direct measurement can be performed in a non-transparent heat pipe. The method is based on the measurement of the capillary limit for different inclination angles. When the heat pipe is tilted in unfavourable conditions, the capillary limit decreases because of the effect of the gravitational pressure drops. The frictional pressure drop and the effective pore radius of the capillary structure can be estimated by assuming that the capillary pressure at the capillary limit is constant whatever the inclination angle (figure 5). This method has been successfully tested on a grooved flat plat heat pipe and validated by means of microscopy measurements (figure 6). However, more studies are required to use this method with other capillary structures, as the assumption of a constant capillary pressure at the capillary limit of the heat pipe is not trivial, especially when boiling can be expected.

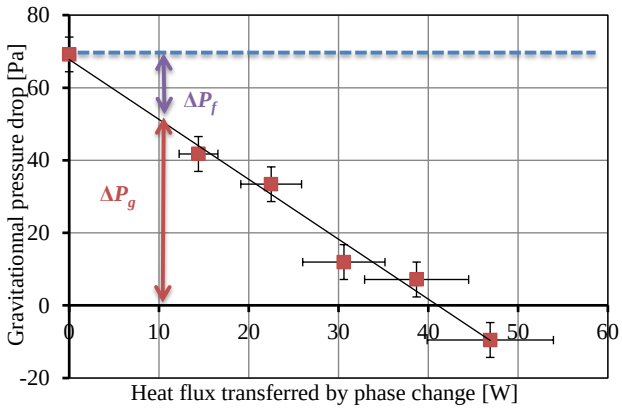

Figure 5 Example of evolution of the gravitational pressure drop as a function of the heat transfer rate transferred by phase change (L_{evap} = 140 mm) [15]

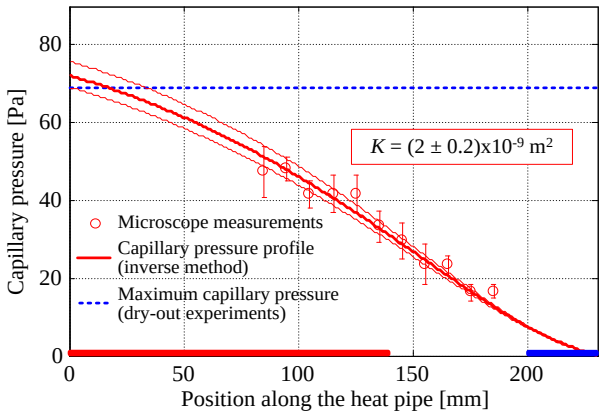

Figure 6 Example of capillary pressure measurement by means of a confocal microscope [15]

Even if a great number of papers are devoted to the determination of the heat pipe performance and/or the capillary structure properties, there is often a need in understanding the phenomena that take place in the heat pipe itself as the models often assume a given heat pipe behavior, which is not always verified experimentally.

FLUID BEHAVIOUR PROBLEMATIC

Heat pipe behaviour and working regime

The performance of a heat pipe often depends on numerous parameters and specific studies focuses on the understanding on the heat pipe behavior itself. For conventional capillary heat pipes, the working condition are bounded by several limits that all lead to a dry-out at the evaporator. For thermosyphons, pulsating heat pipes and loop heat pipes, several working regimes can be observed and recent progress have been made in their characterization. As an example, Kaled *et al.* studied flow regime [16] and transient behavior [17] of a CPL. They concluded that the pseudo-periodic period of the system was affected by the fluid motion and had a direct influence on the pressure drop in the loop.

Working regime is also of a great importance for PHP. Karthikeyan *et al.* [18] studied the self-sustained oscillations in a PHP by means of an infrared camera (figure 7). They characterized the different working regime and their impact on the heat pipe performance.

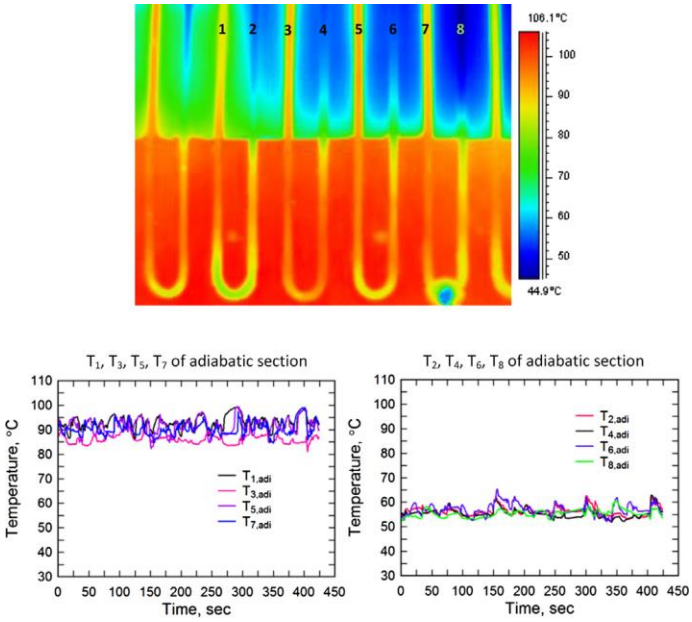

Figure 7 Experimental characterization of the working regime of a PHP by means of a thermal camera [18]

In situ visualization

Thermal measurements help to characterize the heat pipe behavior, but it is often important to deal with the behavior of the working fluid inside the capillary structure itself. Heat pipe are often studied as black boxes and thus no direct observation can be performed inside the system. For ten years, many research teams studied transparent heat pipes, which allows a better understanding of the physical phenomena that take place inside the system. Lips *et al.* [19] observed that boiling could occur at the evaporator of a grooved flat plate heat pipe without preventing the operation of the system. With the same experimental apparatus, they showed that the vapor space thickness had a direct impact on the maximum capillary pressure in the heat pipe [20]. These two phenomena were never taken into account in numerical models, despite their important impact on the heat pipe performance.

A confocal microscope has also been used to measure the pressure drop of the liquid inside the capillary structure for a 1D capillary structure [21] and a 2D capillary structure [22]. These experimental results enabled the validation of the hydrodynamic models for the liquid flow in grooves. However, this technology cannot be used to visualize liquid/vapor interfaces in other capillary structures, as meshes or sintered wicks: the prediction of the pressure drop in this type of capillary structure remains an important challenge.

The confocal microscopy has also been successfully used for the condensing film measurement on a silicon heat pipe [23]. Indeed, the shape of the condensing film is of a great importance

in heat pipes as it affects directly the thermal resistance at the condenser.

The contribution of the confocal microscopy to the heat pipe behaviour knowledge is discussed here as an example, but transparent systems were also widely used for the study of thermosyphons [24], pulsating heat pipes [25] and loop heat pipes [26].

Decoupling of the phenomena

In order to study in detail the liquid-vapor interface shape, some studies focus on a single part of the heat pipe only. For instance, El Achkar *et al.* [27] studied the condensation of n-pentane in a micro-channel that represent the condenser of a LHP. They measured the size and the frequency of the vapour bubbles during the condensation and quantified the sensible heat importance compared to the latent heat of phase change. On the other hand, Mottet *et al.* [28] developed a test bench dedicated to the study of partial dry-out in the evaporator of a LHP. A fictive evaporator is designed and experimental results are compared to model predictions (figure 8).

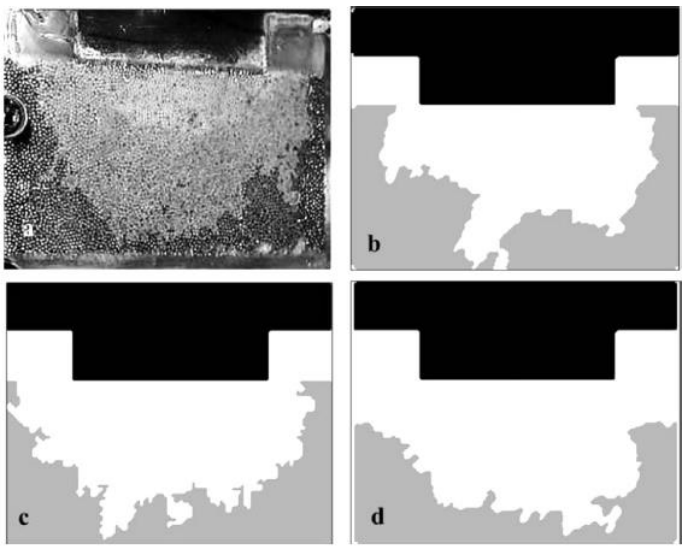

Figure 8 Visualisation and modelling of the vapour region in the evaporator of a LHP [28]

These example of experimental models of a part of a LHP highlight the importance of the direct visualisation in these kinds of systems: the organisation of the liquid in the capillary structure of a heat pipe is far from being trivial and the numerical models are often limited by an imperfect understanding of the fluid behaviour. This lack of knowledge impacts directly the pertinence of the heat pipe design tools as the prediction of their thermal performance depends mainly on the liquid film thickness in the condenser and evaporator.

New fluids

Beside research on the working fluid behaviour, some studies are dedicated to new kind of fluids themselves. The choice of the fluid is indeed of a great importance and it is not so trivial to choose the good fluid for the good technology of heat pipe for a specific application. For instance, MacGregor *et al.* proposed a comparison of different working fluid performances for thermosyphons in order to replace R134a, widely used, but subject to a ban in a close future [29]. Authors also test their prototypes with new refrigerants, as R1234ze, which is found to be an efficient working fluid for loop heat pipes [30]. In a general way, the definition of an efficient working fluid is still a subject of discussion: Launay *et al.* [31] proposed a figure of merit for the working fluid in loop heat pipes, whereas Arab and Abbas proposed a model to predict the thermal performance of a trapezoidal grooved heat pipe when changing the working fluid [32].

Besides new fluids themselves, the heat pipe research mainly focus on two new fluid families: the self-rewetting fluids and the nano-fluids.

The self-rewetting fluids exhibit an increase of its surface tension when its temperature increase. They often consist of a dilute aqueous solution of alcohol: A concentration gradient occurs at the evaporator and the Marangoni effect adds to the temperature effect and helps drain the fluid from the condenser to the evaporator. Firstly studied for space applications [33], self-rewetting fluids have now been successfully tested in conventional heat pipes [34], thermosyphons [35] and even oscillating heat pipes [36]. The self-rewetting fluids have been proved to be potentially efficient, but more studies are still required to precisely predict their behaviour.

A nano-fluid consists on a liquid base in which nanometer-sized particles are incorporated. Depending on their material, the nanoparticles can affect the heat transfer in the fluid. These last years, numerous studies on nano-fluids in heat pipes have been published. In 2012, Liu and Li performed a review of the dedicated studies and concluded that depending on the type of nano-particles, their size and their concentration, nano-fluids could significantly increase the heat pipe performances, both in terms of thermal resistance and of maximum heat removal capacity [37]. The major effect of nano-fluids seems to be the surface structuring at the evaporator, which affects the wettability of the wall, as well as the boiling phenomenon. These conclusions are shared with other review articles published in 2013 [38] and 2014 [39]. Figure 9 shows the number of publications dedicated to nano-fluid in heat pipes according to the database of Web Of Science™.

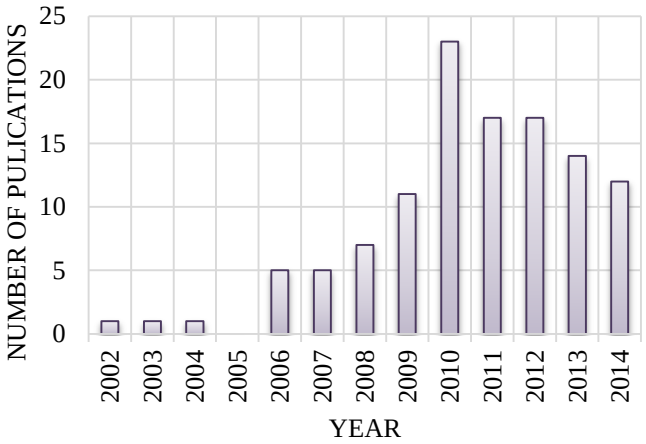

Figure 9 Number of publications dedicated to nano-fluids in heat pipes according to the database of Web Of Science™

The number of paper increased rapidly between 2006 and 2010, but decreases since then. Finally, the studies on nano-fluids can be viewed as studies on liquid-vapour phase change heat transfer on nano-structured surface. If the effect of nano-fluids on heat pipe performance is well admitted, the difficulty of characterizing accurately the causes of this effect limits the understanding and the reproducibility of the phenomena. One can admit that the liquid-vapor phase change heat transfer in a capillary structure are not perfectly well understood even without nano-fluids.

PHASE CHANGE HEAT TRANSFER IN THIN FILMS

Prediction of heat transfer coefficient during evaporation or condensation

The difficulty in predicting the thermal performance of a heat pipe lies in the predominance of heat transfer through very thin liquid film. Numerous studies aim at determining experimentally heat transfer coefficients during condensation or evaporation, but the models fail at reproducing the measurements, even for simple geometries as grooves [40]. In 2010, Khandekar *et al.* pointed that too many fundamental phenomena still need to be understood to achieve a complete model of PHP because of the oscillating character of the Taylor bubble flow [41]. Experimental setups have since been developed to study the evaporation and condensation phenomena in capillary tubes. For instance, Chauris *et al.* studied the evaporation of the thin film deposited by a moving meniscus [42]. They highlighted the phenomena involved in the process and quantified the impact of each phenomena on the global heat transfer. As an example, figure 10 shows the repartition of the energy transferred from the wall to the fluid during the passage of a meniscus. Most of the energy is transferred through the thin liquid film deposited by the meniscus, but the impact of the meniscus itself is far from being negligible. Other recent studies focuses on heat transfer in thin films, but with no direct application to heat pipes. As an example, Kunkelmann *et al.* studied the effect of the three phase contact line velocity on the heat transfer [43]. They also developed a model enabling to predict the main trends of the experimental results.

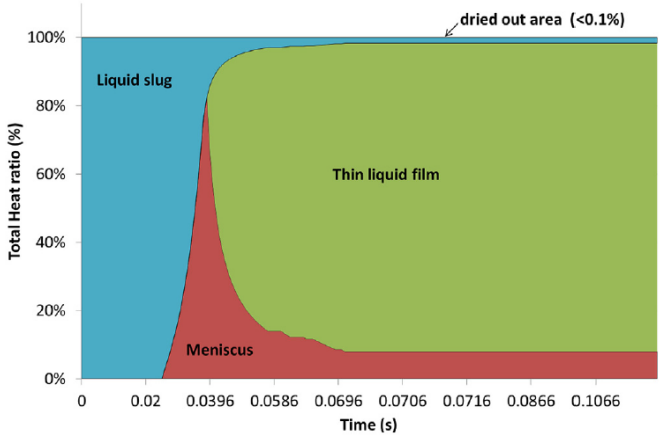

Figure 10 Repartition of the heat transferred from the wall to the fluid during the passage of a meniscus [42]

They concluded that the heat transfer in the contact line zone depend mainly on the micro layer evaporation and on the transient conduction in the wall. At the scale of the liquid thin film, the properties of the wall is indeed found not to be negligible and the coupling of the phenomena is complex.

Example of phenomenological study of a one-branch pulsating heat pipe

To highlight this complexity, a study performed by Rao *et al.* and dedicated to the understanding of a one-branch pulsating heat pipe is detailed in the present section. This paper illustrates the coupling of thermal and hydrodynamic phenomena, which can lead to self-sustained oscillations [44].

Their experimental set-up is detailed in figure 11. It consists of a single vertical and transparent capillary tube closed on one side and connected to a reservoir on the other side. Two transparent water heat exchangers, acting as an evaporator and a condenser, are located along the heat pipe. Depending on the temperatures of the reservoir, the evaporator and the condenser, self-sustained oscillations of the meniscus are observed.

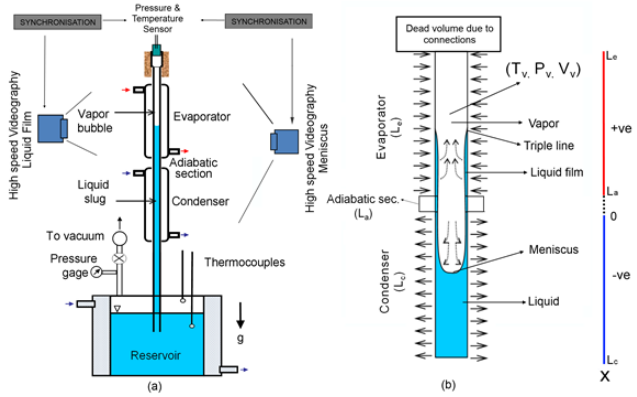

Figure 11 Schematic of the experimental set-up of Rao *et al.* [44]

The authors measured simultaneously the meniscus position, the triple contact line position, the vapour pressure and the vapour temperature. They described the four zone cycle associated to the meniscus oscillation and highlighted the main phenomena involved in the process (figure 12). In the first zone, the meniscus is moving upward in the evaporator zone until reaching its top most position. The vapour pressure increases because of the compression effect. In the second zone, the meniscus moves downwards. The vapour pressure still increases because of the strong evaporation of the thin liquid film left by the meniscus. In the third zone, the meniscus enters the condenser zone. The vapour pressure decreases, but the liquid film is still present and evaporates. The meniscus reaches its first most-bottom position and then moves upwards because of the reservoir pressure, despite the evaporation of the thin liquid film. The vapour pressure still increases and the meniscus moves downward again without having entered in the evaporator zone. It reaches its second most-bottom position. When the meniscus moves upward again (fourth zone), the liquid film has completely evaporated and the vapour pressure is low enough for the meniscus to enter in the evaporator zone. The cycle then repeats itself.

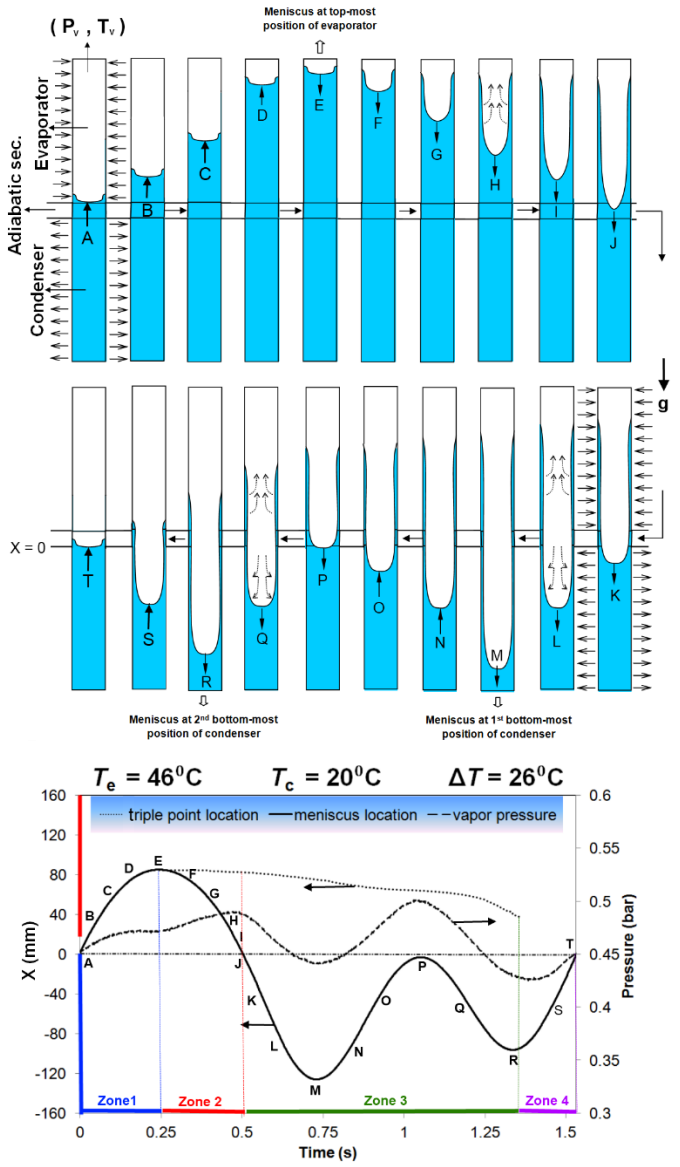

Figure 12 Description of the four zone cycle and the associated phenomena [44]

The observed cycle is thus a result of a balance between the pressure of the reservoir, the variation of pressure due to the compression and expansion phenomena and the variation of pressure due to the change of vapour mass resulting from condensation of evaporation of the fluid. The four zone shape is due to the difference of time scale between the hydrodynamic phenomena and the phase change phenomena. The authors showed that the vapour is always superheated. It enables them to determine the instantaneous mass of vapour and to estimate by a thermal model the rate of evaporation and condensation in different zone of the liquid-vapour interface during a cycle (figure 13). Condensation occurs mainly on the liquid film and evaporation occurs both on the liquid film and the triple contact line. For both evaporation and condensation, the phase change rate is maximum when the meniscus is at its second bottom-most position.

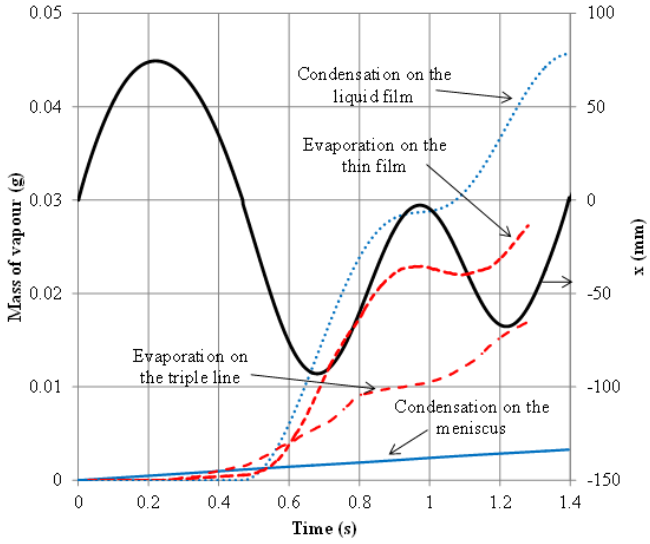

Figure 13 Estimation of the contribution of different phenomenon on the evaporation and condensation rate [44]

This study is a good example of the complexity of the balance between thermal and hydrodynamic phenomena that can occur in a heat pipe. In the case of a pulsating heat pipe, no complete model is able to predict their behaviour, but the progress in the understanding of the phenomena contributes to more realistic models.

SYSTEM MODELING

During the past few years heat pipes models have indeed been improved. Both analytical and numerical models were proposed at the scale either of a single phenomenon or of the system. Concerning conventional heat pipes, two types of studies have been published: the progress in CFD modelling enabled the development of 3D thermal and hydrodynamic models [45], but in parallel, analytical models have also been proposed [46]. The first ones enable a better integration of the heat pipe in a more complex system, whereas the second ones give simple and accurate engineering tools for the design of the heat pipes themselves. Some other specific studies aimed at determining the properties of the wick properties by means of detailed thermal and hydrodynamic model on the pore scale directly [47].

Several studies have been devoted to the modelling of loop heat pipes. Siedel *et al.* proposed a complete review of the steady-state modelling works [48]. They highlighted the high number of models available and noted that most of them are numerical. The same others also proposed in another paper a complete analytical model, requiring a low computational time compared to numerical ones [49]. These models are able to reproduce the experiments, but their limit lies in the lack of knowledge of the wick properties and in the determination of the different thermal resistances involved in the systems. Transient models of LHP have also been proposed, but they still fail in predicting some phenomena [50].

An important part of the modelling worked published the last few years were devoted to pulsating heat pipes. On one side,

the increasing number of experimental databases enabled the development of empirical correlations [51]. On the other side, some 3D CFD models have been proposed [52] and phenomenological models were implemented. They showed a good ability to reproduce the chaotic behaviour of PHPs [53]. In all cases, these models still have to be improved in order to take into account all physical phenomena, especially at the scale of the thin liquid film and the triple contact line. Detailed model already exists to understand these zone, but their experimental validation remains challenging [54].

CONCLUSION

This brief review of recent studies focused on heat pipes enables to highlight the main approaches used by the research teams to increase the understanding of the different type of systems. Both experimental and theoretical works are proposed and the scale of interest of the studies varies from the system size itself to the scale of the very thin liquid film present in the evaporation and condensation zones.

During the past five years, some significant advances have been achieved:

- The understanding of evaporation and condensation phenomena on a capillary scale has been improved, mainly thanks to new systems of visualisation and instrumentation.
- New fluids and new materials have been successfully tested and enable to increase the heat pipe performances.
- Major progresses in the understanding of LHP have now enabled to develop this technology at an industrial scale. The models are now able to predict satisfactory the experiments even if improvements can still be achieved in the prediction of transient behaviour and thermal resistance involved in the systems.
- The more impressive advances are probably dedicated to the PHP. Five years ago, even the main phenomena were not well identified. Models are now almost able to reflect their chaotic behaviour and reliable predictive tools can be expected in the coming few years.

However, several scientific questions still have to be answered:

- The predictive tools strongly depend on the capillary structure properties and on the heat transfer coefficient during condensation and evaporation. Very few progresses have been realized in developing satisfactory models or correlations, even for simple geometries.

- Several phenomena still have to be better understood to be taking into account correctly in the models. Boiling in the capillary structure of a flat heat pipe and coalescence and break-up of liquid slugs and vapor plugs in pulsating heat pipes are only two examples.

- The evaporation and condensation process implying film liquid film are not yet fully understood, and especially the influence of the wall properties on these phenomena.

One can also expect that the progresses in other research fields will bring new tools enabling to improve the current systems. For instance, the progress in high frequency micro-electronic open the way for active control of heat pipes and the continuous researches on new material awaken hopes of real flexible and lightweight heat pipes if the current problem of fluid/material compatibility on plastic heat pipes are solved. Anyway, one can conclude that the study of heat pipes will remain a challenging and exciting topic for the next couple of decades.

REFERENCES

[1] Reay, D., McGlen, R., and Kew, P. *Heat Pipes: Theory, Design and Applications.* Butterworth-Heinemann, Amsterdam u.a., 2013.

[2] Riffat, S. and Ma, X. Recent developments in heat pipe technology and applications: a review. *International Journal of Low-Carbon Technologies 2*, 2 (2007), 162–177.

[3] Maydanik, Y.F., Chernysheva, M.A., and Pastukhov, V.G. Review: Loop heat pipes with flat evaporators. *Applied Thermal Engineering 67*, 1–2 (2014), 294–307.

[4] Fried, S.S., Maydanik, Y.F., and Kozhin, V.A. *Liquid cooled condensers for loop heat pipe like enclosure cooling.* Google Patents, 2013.

[5] Asfia, J.F., Cai, Q., and Chen, C.-L. Multi-layer wick in loop heat pipe. 2014. http://www.google.com/patents/US8720530.

[6] Bonjour, J., Lefevre, F., Sartre, V., and Siedel, B. Improved device for closed-loop heat transport. 2013. http://www.google.com/patents/WO2013174856A1.

[7] Lachassagne, L., Ayel, V., Romestant, C., and Bertin, Y. Experimental study of capillary pumped loop for integrated power in gravity field. *Applied Thermal Engineering 35*, (2012), 166–176.

[8] Lachassagne, L., Bertin, Y., Ayel, V., and Romestant, C. Steady-state modeling of Capillary Pumped Loop in gravity field. *International Journal of Thermal Sciences 64*, (2013), 62–80.

[9] Singh, R., Nguyen, T., and Mochizuki, M. Capillary evaporator development and qualification for loop heat pipes. *Applied Thermal Engineering 63*, 1 (2014), 406–418.

[10] Santos, P.H.D., Bazzo, E., and Oliveira, A.A.M. Thermal performance and capillary limit of a ceramic wick applied to LHP and CPL. *Applied Thermal Engineering 41*, (2012), 92–103.

[11] Ameli, M., Agnew, B., Leung, P.S., et al. A novel method for manufacturing sintered aluminium heat pipes (SAHP). *Applied Thermal Engineering 52*, 2 (2013), 498–504.

[12] Hansen, G., N\a ess, E., and Kristjansson, K. Sintered Nickel Powder Wicks for Flat Vertical Heat Pipes. *Energies 8*, 4 (2015), 2337–2357.

[13] Ababneh, M.T., Gerner, F.M., Chamarthy, P., Bock, P. de, Chauhan, S., and Deng, T. Thermal-Fluid Modeling for High Thermal Conductivity Heat Pipe Thermal Ground Planes. *Journal of Thermophysics and Heat Transfer 28*, 2 (2014), 270–278.

[14] Iverson, B.D., Davis, T.W., Garimella, S.V., North, M.T., and Kang, S.S. Heat and mass transport in heat pipe wick structures. *Journal of Thermophysics and Heat Transfer 21*, 2 (2007), 392–404.

[15] Revil-Baudard, L. and Lips, S. A non-invasive method for thermal and hydrodynamic characterisation of flat plate heat pipes. *9th International conference on Boiling and condensation Heat Transfer*, (2015).

[16] Miscevic, M., El Achkar, G., Lavieille, P., Kaled, A., and Dutour, S. About flow regime and heat transfer in low diameter condenser of LHP and CPL. *16th International Heat Pipe Conference*, (2012).

[17] Kaled, A., Dutour, S., Platel, V., Lachassagne, L., and Ayel, V. A theoretical analysis of the transient behavior of a cpl for terrestrial application. *16th International Heat Pipe Conference (16th IHPC)*, (2012).

[18] Karthikeyan, V.K., Khandekar, S., Pillai, B.C., and Sharma, P.K. Infrared thermography of a pulsating heat pipe: Flow regimes and multiple steady states. *Applied Thermal Engineering 62*, 2 (2014), 470–480.

[19] Lips, S., Lefèvre, F., and Bonjour, J. Nucleate boiling in a flat grooved heat pipe. *International Journal of Thermal Sciences 48*, 7 (2009), 1273–1278.

[20] Lips, S., Lefèvre, F., and Bonjour, J. Combined effects of the filling ratio and the vapour space thickness on the performance of a flat plate heat pipe. *International Journal of Heat and Mass Transfer 53*, 4 (2010), 694–702.

[21] Lips, S., Lefèvre, F., and Bonjour, J. Physical mechanisms involved in grooved flat heat pipes: Experimental and numerical analyses. *International Journal of Thermal Sciences 50*, 7 (2011), 1243–1252.

[22] Lips, S., Lefèvre, F., and Bonjour, J. Thermohydraulic Study of a Flat Plate Heat Pipe by Means of Confocal Microscopy: Application to a 2D Capillary Structure. *Journal of Heat Transfer 132*, (2010), 019008.

[23] Lefèvre, F., Rullière, R., Lips, S., and Bonjour, J. Confocal Microscopy for Capillary Film Measurements in a Flat Plate Heat Pipe. *Journal of Heat Transfer 132*, 3 (2010), 031502.

[24] Smith, K., Kempers, R., Robinson, A.J., and Siedel, S. Flow Visualisation in a Transparent Thermosyphon: Influence of Internal Pressure. Begellhouse (2014).

[25] Ji, Y., Liu, G., Ma, H., Li, G., and Sun, Y. An experimental investigation of heat transfer performance in a polydimethylsiloxane (PDMS) oscillating heat pipe. *Applied Thermal Engineering 61*, 2 (2013), 690–697.

[26] Xu, J., Zhang, L., Xu, H., Zhong, J., and Xuan, J. Experimental investigation and visual observation of loop heat pipes with two-layer composite wicks. *International Journal of Heat and Mass Transfer 72*, (2014), 378–387.

[27] El Achkar, G., Lavieille, P., and Miscevic, M. Loop heat pipe and capillary pumped loop design: About heat transfer in the isolated bubbles zone of condensers. *Applied Thermal Engineering 33-34*, (2012), 253–257.

[28] Mottet, L., Coquard, T., and Prat, M. Three dimensional liquid and vapour distribution in the wick of capillary evaporators. *International Journal of Heat and Mass Transfer 83*, (2015), 636–651.

[29] MacGregor, R.W., Kew, P.A., and Reay, D.A. Investigation of low Global Warming Potential working fluids for a closed two-phase thermosyphon. *Applied Thermal Engineering 51*, 1–2 (2013), 917–925.

[30] Yeo, J., Yamashita, S., Hayashida, M., and Koyama, S. A Loop Thermosyphon Type Cooling System for High Heat Flux. *Journal of Electronics Cooling and Thermal Control 4*, 04 (2014), 128.

[31] Launay, S., Sartre, V., and Bonjour, J. Selection criteria for fluidic and geometrical parameters of a LHP based on analytical approach. *Proc. 15th International Heat Pipe Conference*, (2010).

[32] Arab, M. and Abbas, A. A model-based approach for analysis of working fluids in heat pipes. *Applied Thermal Engineering 73*, 1 (2014), 751–763.

[33] Savino, R., Di Paola, R., Cecere, A., and Fortezza, R. Self-rewetting heat transfer fluids and nanobrines for space heat pipes. *Acta Astronautica 67*, 9–10 (2010), 1030–1037.

[34] Senthilkumar, R., Vaidyanathan, S., and Sivaraman, B. Comparative study on heat pipe performance using aqueous solutions of alcohols. *Heat and Mass Transfer 48*, 12 (2012), 2033–2040.

[35] Karthikeyan, M., Vaidyanathan, S., and Sivaraman, B. Heat transfer analysis of two-phase closed thermosyphon using aqueous solution of n-butanol. *International Journal of Engineering and Technology 3*, 6 (2013), 661–667.

[36] Hu, Y., Liu, T., Li, X., and Wang, S. Heat transfer enhancement of micro oscillating heat pipes with self-rewetting fluid. *International Journal of Heat and Mass Transfer 70*, (2014), 496–503.

[37] Liu, Z.-H. and Li, Y.-Y. A new frontier of nanofluid research–Application of nanofluids in heat pipes. *International Journal of Heat and Mass Transfer 55*, 23 (2012), 6786–6797.

[38] Sureshkumar, R., Mohideen, S.T., and Nethaji, N. Heat transfer characteristics of nanofluids in heat pipes: A review. *Renewable and Sustainable Energy Reviews 20*, (2013), 397–410.

[39] Alawi, O.A., Sidik, N.A.C., Mohammed, H.A., and Syahrullail, S. Fluid flow and heat transfer characteristics of nanofluids in heat pipes: A review. *International Communications in Heat and Mass Transfer 56*, (2014), 50–62.

[40] Lips, S., Lefevre, F., and Bonjour, J. Investigation of evaporation and condensation processes specific to grooved flat heat pipes. *Frontiers in heat pipes 1*, 2 (2010), 023001–1 ; 023001–8.

[41] Khandekar, S., Pnigrahi, P.K., Lefevre, F., and Bonjour, J. Local hydrodynamics of flow in a pulsating heat pipe: a review. *Frontiers in heat pipes 1*, 2 (2010), 023001–1 ; 023001–20.

[42] Chauris, N., Ayel, V., Bertin, Y., and Romestant, C. Evaporation of a liquid film deposited on a capillary heated tube: Experimental analysis by infrared thermography of its thermal footprint. *International Journal of Heat and Mass Transfer 86*, (2015), 492–507.

[43] Kunkelmann, C., Ibrahem, K., Schweizer, N., Herbert, S., Stephan, P., and Gambaryan-Roisman, T. The effect of three-phase contact line speed on local evaporative heat transfer: Experimental and numerical investigations. *International Journal of Heat and Mass Transfer 55*, 7-8 (2012), 1896–1904.

[44] Rao, M., Lefèvre, F., Khandekar, S., and Bonjour, J. Heat and mass transfer mechanisms of a self-sustained thermally driven oscillating liquid-vapour meniscus. .

[45] Wang, J.-C. 3-D numerical and experimental models for flat and embedded heat pipes applied in high-end VGA card cooling system. *International Communications in Heat and Mass Transfer 39*, 9 (2012), 1360–1366.

[46] Lips, S. and Lefèvre, F. A general analytical model for the design of conventional heat pipes. *International Journal of Heat and Mass Transfer 72*, (2014), 288–298.

[47] Ranjan, R., Patel, A., Garimella, S.V., and Murthy, J.Y. Wicking and thermal characteristics of micropillared structures for use in passive heat spreaders. *International Journal of Heat and Mass Transfer 55*, 4 (2012), 586–596.

[48] Siedel, B., Sartre, V., and Lefèvre, F. Literature review: Steady-state modelling of loop heat pipes. *Applied Thermal Engineering 75*, (2015), 709–723.

[49] Siedel, B., Sartre, V., and Lefèvre, F. Complete analytical model of a loop heat pipe with a flat evaporator. *International Journal of Thermal Sciences 89*, (2015), 372–386.

[50] Nishikawara, M., Nagano, H., and Kaya, T. Transient thermo-fluid modeling of loop heat pipes and experimental validation. *Journal of Thermophysics and Heat Transfer 27*, 4 (2013), 641–647.

[51] Qu, J. and Wang, Q. Experimental study on the thermal performance of vertical closed-loop oscillating heat pipes and correlation modeling. *Applied Energy 112*, (2013), 1154–1160.

[52] Lin, Z., Wang, S., Shirakashi, R., and Winston Zhang, L. Simulation of a miniature oscillating heat pipe in bottom heating mode using CFD with unsteady modeling. *International Journal of Heat and Mass Transfer 57*, 2 (2013), 642–656.

[53] Nikolayev, V.S. A Dynamic Film Model of the Pulsating Heat Pipe. *Transactions of the ASME-C-Journal of HeatTransfer 133*, 8 (2011), 081504.

[54] Nikolayev, V.S. Dynamics of the triple contact line on a nonisothermal heater at partial wetting. *Physics of fluids 22*, 8 (2010), 082105.

EFFECTS OF GEOMETRY AND FLUID PROPERTIES DURING CONDENSATION IN MINICHANNELS: EXPERIMENTS AND SIMULATIONS

Del Col D.*, Bortolin S., Toninelli P.
University of Padova, Department of Industrial Engineering
Via Venezia, 1 –35131, Padova, Italy
*Author for correspondence. E-mail: davide.delcol@unipd.it

ABSTRACT

The present paper aims at providing a review of the condensation process inside micro and minichannels, above all at low mass fluxes, when we can expect more discrepancies from conventional channels.

At high mass flux, the condensation in minichannels is expected to be shear stress dominated. Therefore, models originally developed for conventional channels could still do a good job in predicting the heat transfer coefficient. Besides, at high mass flux, the effect of the channel shape may not be significant, due to the importance of the shear stress at the liquid-vapour interface in comparison with the capillary forces. When the mass flow rate decreases, the condensation process in microchannels starts to display differences with the same process in macro-channels.

With the purpose of investigating condensation at these operating conditions, new experimental data are here reported and compared with data already published in the literature. In particular, heat transfer coefficients have been measured during R134a and R1234ze(E) condensation inside circular and square cross section minichannels at mass velocity ranging between 65 and 200 kg m^{-2} s^{-1}. These new data are compared with those of R32, R245fa, R290, R152a to show the effect of channel shape and fluid properties and to assess the applicability of correlations for macroscale condensation. For this purpose, a new criterion is presented based on the Weber number.

The present experimental data are also compared against three-dimensional VOF simulations of condensation in minichannels with circular and square cross section. This comparison allows to get an insight into the process and evaluate the main heat transfer mechanisms.

INTRODUCTION

Nowadays miniaturization has become a key word in heat transfer research allowing the realization of new heat exchangers with high efficiency, reduced dimensions, high area/volume ratio and low refrigerant charge. In particular, condensation inside minichannels has received considerable attention because of its wide application areas such as heat pipes, micro-heat exchangers for electronic equipment, Rankine cycles and automotive applications. In air-cooled condensers of domestic air conditioning units and heat pumps, fin-and-tube heat exchanger is the usual geometry (tube diameter ranging between 6 and 10 mm) but the utilization of multiport minichannels is expected to increase being the refrigerant charge reduction a central issue in such equipments [1]. In fact, reducing the amount of fluid is very important for safety reasons when using natural refrigerants and for limitation of greenhouse gases emissions when using halogenated refrigerants. On the other hand, miniaturization of systems introduces new challenges and this is the reason why condensation heat transfer in minichannels requires more research.

Currently, there is not a well established criterion to define the transition from macro to microscale condensation. In a recent paper Nema et al. [2], starting from a previous visualization study by Coleman and Garimella [3] (R134a, round and square tubes with diameters ranging from 1 to 4.91 mm, G = 150-750 kg $m^{-2}s^{-1}$) developed dimensionless transition criteria to distinguish between the important flow regimes. The transition between macro and microscale (i.e the relative importance of surface tension and gravity) is accounted for by introducing a critical Bond number. For example, in case of R134a condensing at 40°C saturation temperature inside a 1 mm diameter tube, the Bond number is Bo=1.8 and the critical Bond number is Bo_{cr} =3.8; therefore surface tension is expected to play a non-negligible role. For Bond number below the critical value, four different types of flow have been observed by the authors: dispersed, annular film, intermittent/annular film and intermittent; the wavy flow regime was not observed. Many more studies on flow patterns have been published afterwards; although no general flow regime map is available for condensation in minichannels, one important result has been repeatedly reported which is the increased importance of the annular flow regime at the expense of stratified and wavy stratified flow.

It should be noticed that there are some working conditions ($Bo<Bo_{cr}$ and high mass velocities) at which empirical correlations available in the literature, and developed using data from round conventional-size pipes (e.g. Cavallini et al. [4]), predict the condensation heat transfer coefficient with a degree of accuracy suitable for the design of heat exchangers (Cavallini et al. [5], Del Col et al. [6], Del Col et al. [7]). This fact can be explained considering that at high mass velocity the flow is mostly annular and the condensation heat transfer is dominated by vapour shear stress on the liquid film: hence correlations that do not consider surface tension can be successfully applied. Starting from these considerations, two

different regions (respectively high and low mass flux) can be individuated, each of them showing peculiar characteristics of the condensation heat transfer coefficient. At high mass flux, (e.g. $G \geq 400$ kg m^{-2} s^{-1} for of R134a in a 1 mm channel), the main features are:

- Strong influence of the mass flux on the heat transfer coefficient (Bandhauer et al. [8], Matkovic et al. [9], Del Col et al. [6], Liu et al. [10], Sakamatapan et al. [11]).
- Negligible difference of the cross-sectional average heat transfer coefficient between round and square cross section channels ([6], [10]). As reported in Bortolin et al. [12] the shape of the liquid-vapour interface is affected by surface tension, but the average heat transfer coefficient is governed by vapour shear stress.
- No major effect of gravity and channel inclination (Del Col et al. [13]).
- No major difference between macro-scale and micro-scale modeling (models for macro-scale condensation still apply).
- No influence of wall-to-saturation temperature difference [9].

At low mass flux, (e.g. $G \leq 200$ kg m^{-2} s^{-1} for R134a in a 1 mm diameter channel) the main features are:

- Low effect of the mass flux on the heat transfer coefficient (experimental data of Del Col et al. [7] with R1234ze(E) at G = 100-200 kg m^{-2} s^{-1}).
- Stratified flow in round minichannels, with some influence of gravity and inclination (Da Riva and Del Col [14], Marchuk et al. [15], Del Col et al. [13]).
- Flatter heat transfer coefficient vs vapor quality profile as compared to high mass flux conditions.
- Enhancement of heat transfer coefficients in square channels as compared to the round ones (Del Col et al. [6] and Liu et al. [10].
- Models developed for macroscale display in general a lower accuracy at low mass fluxes, especially in square minichannels.

It is clear as, at low mass velocity, other forces, such as surface tension, may play a relevant role, or even be the dominant ones, and a difference between micro-scale and macro-scale heat transfer, as well as an effect of cross sectional shape may exist. Therefore, such conditions are of great interest but unfortunately the low mass flux conditions are also the least investigated, mainly because it is a real challenge to perform measurements of heat transfer coefficient with low experimental uncertainty when the heat flow rate is in the order of few watts. An attempt to account for the relative influence of shear, gravity and surface tension forces was recently made by Garimella et al. [16]. They developed a model for the prediction of the heat transfer coefficient. Two flow zones were designated: shear/gravity dominated (Zone I) and shear/surface tension dominated (Zone II). In Zone I, transition from annular to wavy/annular flow is considered, while in Zone II, the annular to intermittent/annular transition is modelled. Heat transfer models were developed for each regime.

In the recent years, more and more work has been done to develop numerical models of condensation in minichannels that should be able to simulate the heat transfer process resolving momentum and energy equations and thus independent of the particular geometry or set of fluid properties. While empirical correlations are in general specific to a given pipe geometry, theoretical and numerical models could in principle be extended to any non-conventional geometry. Unfortunately, in the present status of the art, no numerical model available in the literature has been fully validated against an experimental data set covering a complete range of fluids, operating conditions, channel dimensions and geometries. Besides, depending on the particular model, calculation time can be very long, reducing its practical applicability. Provided that an appropriate validation is performed, numerical models could be extremely interesting not only for the prediction of the heat transfer coefficient, but also for a better general understanding of the condensation phenomena, since they allow an "insight view" for a qualitative analysis (e.g. three-dimensional distribution of local heat transfer coefficient and condensate film thickness), which is almost impossible to achieve experimentally without affecting the phenomenon itself.

Wang and Rose [17] were the first researchers to report an extensive theoretical study of film condensation in square and triangular minichannels over the mass flux range 100 kg m^{-2} s^{-1} < G < 1300 kg m^{-2} s^{-1}, covering different channel sizes in the range between 0.5 and 5 mm, and refrigerants R134a, R22 and R410A; an analogous study regarding circular minichannels was presented in Wang and Rose [18]. In their work, the condensate film is treated assuming laminar flow and neglecting inertia and convection terms (as in the classical Nusselt theory) but, beside gravity, surface tension is also taken into account, while the shear stress on the condensate surface due to the vapour flow is estimated by means of an empirical correlation. The model was further extended in Wang and Rose [19] including ammonia, R152a, propane and carbon dioxide. For all the refrigerants considered, the condensation heat transfer coefficient in microchannels is claimed to be constant for a large part of the channel length, independently of mass flux and vapour quality: the heat transfer is claimed to be controlled in this region only by surface tension and viscosity.

Another model to predict laminar annular film condensation heat transfer in mini and microchannels and based on a finite volume formulation of the Navier-Stokes and energy equations for the liquid phase has been developed by Nebuloni and Thome [20]. Steady-state results of R134a condensation heat transfer coefficient and condensate film thickness were presented for circular, elliptical, flattened and flower channel shapes with hydraulic diameter ranging from 10 μm up to 1 mm. The model by Nebuloni and Thome [20] is reported to display the same qualitative trends (dependence on wall subcooling, mass flux, channel size and fluid properties) as in Wang and Rose [17]; however, in the model by Nebuloni and Thome [20], it is explicitly reported to be valid only for annular or semi-annular condensation with laminar liquid film. The model has been validated against measurements and is reported to predict the experimental data in the non-intermittent flow regime within 20% deviation.

A new theoretical model for the prediction of laminar film convective condensation heat transfer of pure vapour inside a circular tube with different diameters has been developed by Marchuk et al. [15]. This model includes the effects of the surface tension force, gravity force, and shear stress at the vapour-liquid interface. The motion equations of the condensed

liquid are solved with the approximation of the lubrication theory. The model allows calculating the condensate film thickness across the circular tube, as well as predicting the distribution of the liquid along the tube. The theoretical model has been validated against experimental results. Numerical simulations during condensation of saturated ethanol vapour in a circular tube with diameter from 1 to 5 mm have been performed. The numerical calculations show that the heat transfer coefficient decreases significantly with the increase in the tube diameter. Furthermore, simulations have been run at three different gravity levels (0, 10 and 100 m s^{-2}): the analysis shows that the heat transfer coefficient in the horizontal case increases with the growth of the gravity level. Instead, the gravity influence on the heat transfer coefficient at the initial part of the condenser tube is insignificant due to the annular flow regime with thin liquid film.

Ganapathy et al. [21] presented numerical two-dimensional unsteady simulations of R134a condensation in a 100 μm diameter microchannel. The vapour-liquid flow was modelled by a finite volume method-based implementation of the VOF approach. Their numerical formulation was implemented in the commercial CFD code FLUENT. A single microchannel was modelled as a two-dimensional geometry in the form of a rectangular domain. Simulations have been run at mass flux between 245 and 615 kg m^{-2} s^{-1} and heat flux varying from 200 to 800 kW m^{-2} , reporting around 20% mean absolute error for the Nusselt number as compared to the Shah [22] correlation. In addition, predicted condensation flow regimes (annular, transition, intermittent) have been qualitatively compared against experimental visualization, showing a good agreement.

Bortolin et al. [12] presented a study of R134a condensation in a single horizontal 1 mm i.d. minichannel with circular and square cross section at high mass flux. By the comparison between VOF simulations and experimental data, the authors highlighted the influence of interfacial shear stress on the heat transfer coefficient. In fact, at high mass flux, the interfacial shear stress effects are more important than surface tension and gravity ones, so the liquid film turbulence becomes more significant than the liquid film distribution. For this reason, at these mass velocities, the heat transfer coefficients in circular and square minichannels are shown to be approximately the same. At low mass flux, instead, the interfacial shear stress effect is less important and the liquid flow is expected to be laminar. In this case, the liquid film distribution controls the heat transfer during condensation: surface tension and gravity forces play a key-role to drive the liquid film inside the minichannel. The gravity force is responsible for the liquid film thickness increase at the bottom of the circular minichannel, while in the square minichannel the surface tension forces can be more important than gravity due to the presence of corners. In fact, in a square cross section channel, the surface tension pulls the liquid toward the corners, leading to a thinner liquid film at flat sides and, therefore, to a lower local thermal resistance.

Numerical investigation of steam condensation in a non-circular microchannel (80-250 μm hydraulic diameter) was conducted by El Mghari et al. [23]. Results are given for different microchannels shapes, aspect ratios (2, 3, 4), and for various mass fluxes and contact angles. Reducing the microchannel hydraulic diameter from 250 to 80 μm reduces the condensate film thickness and increases the average heat transfer coefficient up to 39% for the same mass flux. It was concluded that the condensation average heat transfer coefficient increases with aspect ratio for rectangular microchannels. The lowest average Nusselt numbers are obtained for the square microchannel. It should be noticed that such simulations seem not to be able to predict the interface inflection point (meniscus) that is reported at high vapour quality in Wang and Rose [19] and in Bortolin et al. [12].

In a recent work, Antonsen and Thome [24] extended the code previously developed by Nebuloni and Thome [20] to condensing annular flows with turbulent liquid films. Turbulence is taken into account by implementing the algebraic model for turbulent eddy diffusivities for momentum and for heat developed by Cioncolini and Thome [25]. The latter assumes the liquid film shear stress is a function of the liquid film Weber number and hence only the dimensionless liquid film thickness is needed to calculate the eddy diffusivities. This allows the use of mean flow equations for the liquid film and hence it is not necessary to radially discretize the liquid film, thus saving computational time.

Even though much work has been done on numerical modelling, most of the condensation simulations are performed under steady state conditions, and thus neglecting all possible instabilities and non-steady flows, such as wavy and slug and plug two-phase flows. Further developments could come from unsteady simulations which would allow to investigate the full range of possible flow patterns and condensation mechanisms.

Considering the lack of experimental data at low mass velocities and the importance of microscale effects at such conditions, in the present work condensation tests and simulations address exactly these operating range. R134a condensation tests inside a 0.96 mm circular channel and inside 1.23 mm square channel are run at mass velocity ranging between 65 and 200 kg m^{-2} s^{-1}. Furthermore, the new low-GWP fluid R1234ze(E) has been investigated in the square minichannel at mass velocity from 100 to 400 kg m^{-2} s^{-1}. Beside experiments, three-dimensional simulations using the VOF method have been performed at low mass flux.

NOMENCLATURE

Bo	[-]	$[(\rho_L-\rho_V)gD_h^2]/\sigma$
Bo_{cr}	[-]	$[\rho_L/(\rho_L-\rho_V)-\pi/4]^{-1}$
D_h	[m]	Hydraulic diameter
e_p	[%]	Percentage deviation, $e_p=100*(HTC_{CALC}-HTC_{EXP})/HTC_{EXP}$
e_R	[%]	Average deviation, $e_R=(1/N_p)\sum e_p$
g	[m s^{-2}]	Acceleration due to gravity
G	[kg $m^{-2}s^{-1}$]	Mass flux
HTC	[W $m^{-2}K^{-1}$]	Cross-sectional average heat transfer coefficient
J_V	[-]	$xG/[gD_h\rho_V(\rho_L-\rho_V)]^{0.5}$
N_p	[-]	Number of data points
p	[bar]	Pressure
$t+$	[-]	Dimensionless average liquid film thickness
U_{VS}	[m s^{-1}]	xG/ρ_V
U_{LS}	[m s^{-1}]	$(1-x)G/\rho_L$
We	[-]	$\rho_V(U_{VS}-U_{LS})^2D_h/\sigma$
x	[-]	Vapour quality
X_{tt}	[-]	$(\mu_L/\mu_V)^{0.1}(\mu_V/\mu_L)^{0.5}[(1-x)/x]^{0.9}$

Greek characters

α_t^+	[-]	Dimensionless turbulent eddy diffusivity for heat
λ	[W m^{-1}K^{-1}]	Molecular thermal conductivity
μ	[Pa s]	Molecular dynamic viscosity
$\upsilon+$	[-]	Dimensionless turbulent eddy diffusivity for momentum
ρ	[kg m^{-3}]	Density
σ	[N m^{-1}]	Surface tension
σ_N	[%]	Standard deviation, $\sigma_N=\{[\sum(e_p-e_R)^2]/(N_p-1)\}^{0.5}$
τ_W	[Pa]	Wall shear stress

Subscripts

CALC	Calculated
circ	Circular
EXP	Experimental
L	Liquid
S	Saturation
sq	Square
V	Vapour
W	Wall

EXPERIMENTAL DATA

New experimental data have been measured during condensation using two different test sections consisting respectively of a 0.96 mm diameter single circular channel and a 1.23 mm hydraulic diameter square cross section channel. Each test section is made of two counter flow heat exchangers: a pre-section and a measuring section. In the pre-section, the refrigerant coming from the evaporator is desuperheated and partially condensed to achieve the desired vapor quality, while in the second one local heat transfer coefficient measurements are collected during the condensation process. Two stainless steel adiabatic sectors are located at the ends of the measuring section providing a place for the measurement of refrigerant temperature and pressure. The presence of both temperature and pressure transducers at the inlet of the measuring section allows a check of the saturation temperature during condensation tests. A refrigerated thermal bath is used to provide the water entering the measuring section and the pre-section at desired temperature.

Two different distilled water loops serve independently the pre-section and the measuring sector and each of them is provided with a flow regulating valve, which allows to set the mass flow rate measured by a dedicated Coriolis effect mass flow meter. The wall and water temperatures are gauged by thermocouples and the water temperature gains are measured by multi-junction copper-constantan thermopiles. A detailed description of the present test rig and test section is reported by Matkovic et al. [9] for the 0.96 mm circular minichannel and by Del Col et al. [6] for the 1.23 mm square minichannel. Data reduction is described in detail in Del Col et al. [7].

Heat transfer coefficients measured during R134a condensation inside the 0.96 mm circular channel (mass velocity ranging from 65 kg m^{-2}s^{-1} to 200 kg m^{-2}s^{-1}) and inside the 1.23 mm square channel (G = 65 kg m^{-2}s^{-1}) are reported in Fig.1, enlarging the mass flux range of the data set presented in Del Col and co-workers [13]. The saturation temperature is equal to 40°C for all the data.

Condensation has been also investigated with the halogenated olefin R1234ze(E) inside the square minichannel with mass velocity between 100 kg m^{-2} s^{-1} and 400 kg m^{-2} s^{-1} and 40°C saturation temperature (Fig. 2). For the sake of comparison, the experimental data by Del Col et al. [7] taken inside the circular minichannel are reported.

Considering Figs. 1-2, at constant mass velocity, the heat transfer coefficient is found to increase with vapor quality, but the slope of the HTC-x curve is lower at low mass velocity values. In addition, Fig. 2 shows that for G < 200 kg m^{-2}s^{-1} the influence of mass velocity on the heat transfer is reduced.

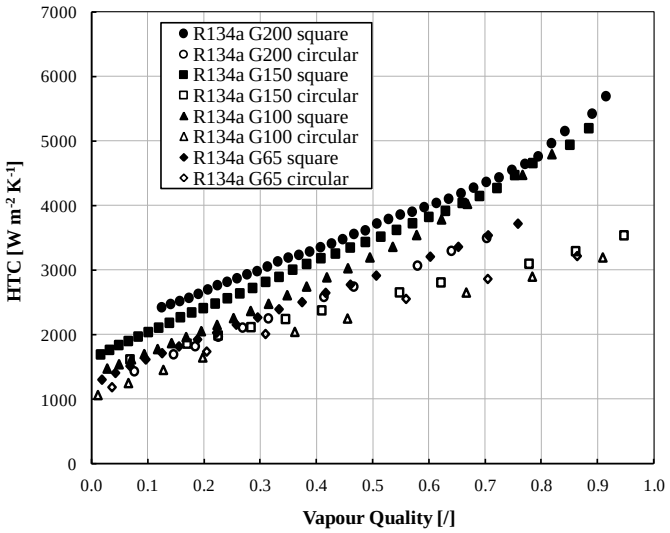

Figure 1 New experimental data and values reported by Del Col et al. [13] of local heat transfer coefficient during R134a condensation inside circular and square minichannels at varying mass flux G [kg m^{-2} s^{-1}].

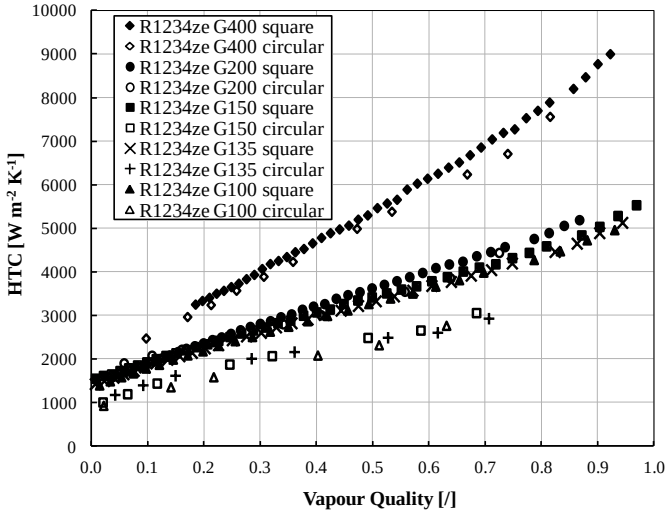

Figure 2 New experimental data and values reported by Del Col et al. [7] of local heat transfer coefficient during R1234ze(E) condensation inside square and circular minichannels at varying mass flux G [kg m^{-2} s^{-1}].

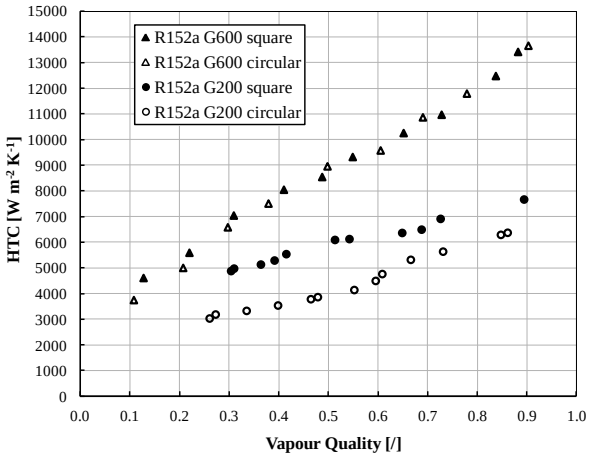

Figure 3 Effects of vapour quality and channel geometry on the heat transfer coefficients during R152a condensation at G = 600 kg m^{-2} s^{-1} and at G = 200 kg m^{-2} s^{-1} (data by Liu et al. [10]).

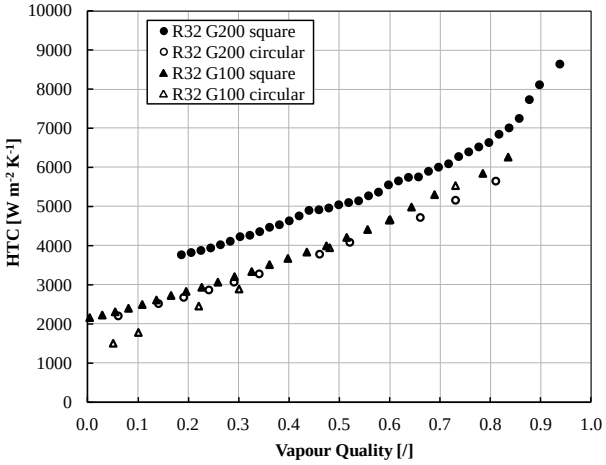

Figure 4 Effects of vapour quality and channel geometry on the heat transfer coefficients during R32 condensation at low mass velocity.

Effect of the cross section shape

As reported in previous works (Del Col et al. [6], Liu et al. [10]) at high mass flow rate, (e.g. $G \geq$ 400 kg m^{-2} s^{-1}) the heat transfer coefficient is not significantly affected by the channel shape while it only depends on the channel hydraulic diameter. In Fig. 3 experimental data during R152a condensation taken inside a 1.152 mm circular channel and in a 0.952 mm square channel by Liu et al. are reported. At G = 600 kg m^{-2} s^{-1} the square and circular channel display roughly the same heat transfer coefficient. This behaviour is confirmed also in the present authors' data with R1234ze(E) at G = 400 kg m^{-2} s^{-1} (Fig. 2). When moving to lower values of mass velocity (Figs. 1-4) there is a clear increase of the heat transfer coefficient in the square channel as compared to the circular one for all the four fluids here presented (R134a, R1234ze, R152a, R32). This heat transfer enhancement is due to the presence of the corners, because the surface tension pulls the liquid toward the corners, leading to a thinner liquid film at flat sides and, therefore, to a lower average thermal resistance. With the aim of better evaluating the heat transfer coefficient increase, in Fig. 5 the ratio of heat transfer coefficient in the square channel to the one in the circular minichannel is reported versus vapour quality at different mass velocities. It can be observed that there is a value of mass velocity at around 200 kg m^{-2} s^{-1} at which the channel shape effect, due to surface tension, becomes relevant. A further reduction in mass velocity can cause first an augmentation of such heat transfer coefficient ratio up to a maximum; at even lower mass flux the percentage difference becomes smaller (see for instance R32 data).

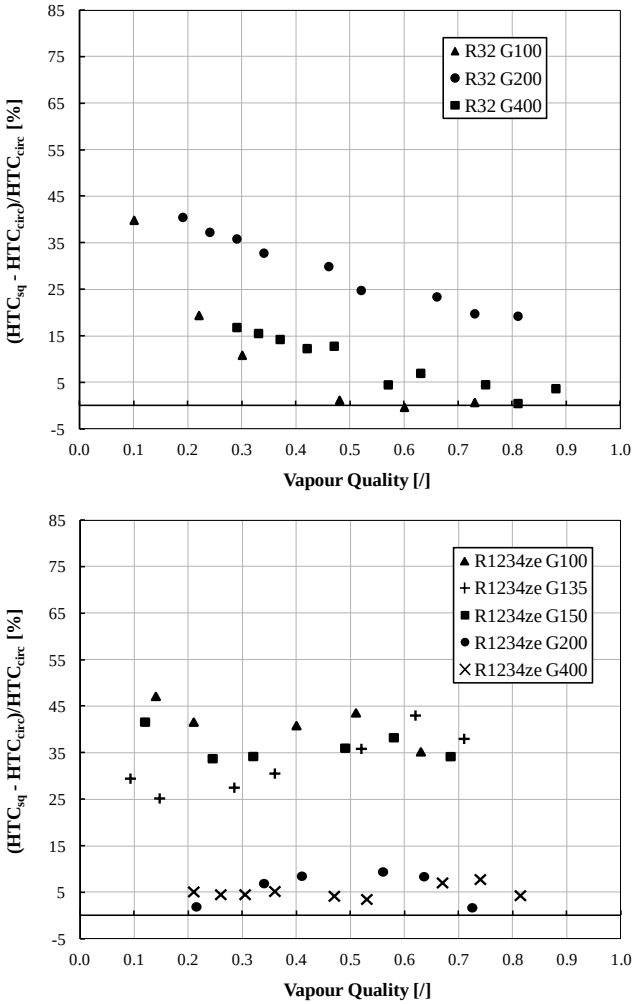

Figure 5 Percentage increase of local heat transfer coefficient in the square channel compared to the one in the circular at mass flux between 100 and 400 kg m^{-2}s^{-1} and 40°C saturation temperature. Top: data of R32 by Del Col at al. [13] and Cavallini et al. [5]. Bottom: data of R1234ze(E) by present authors and by Del Col et al. [7].

Effect of fluid properties

In order to highlight the influence of fluid properties on the condensation process at low mass velocity, R245fa data by Cavallini et al. [5] and R290 data by Del Col et al. [26] are also plotted in Fig. 6. The properties of all these refrigerants are listed in Table 1.

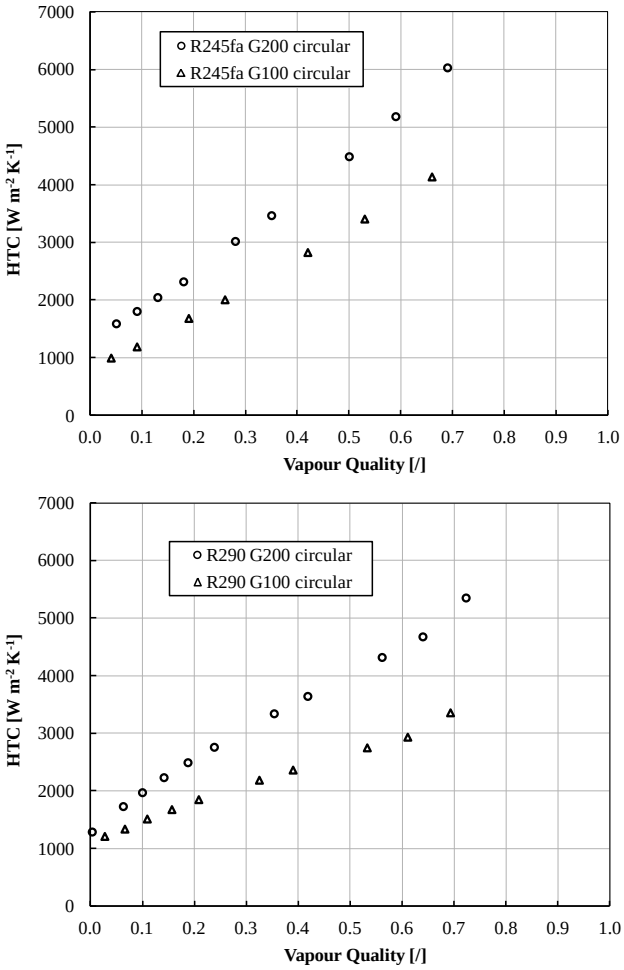

Figure 6 Local heat transfer coefficient during condensation inside the circular minichannel at varying mass flux G [kg m^{-2} s^{-1}]. Top: data of R245fa by Cavallini et al. [5]; bottom: data of R290 by Del Col et al. [26].

Table 1 Properties of saturated R32, R134a, R1234ze(E), R245fa and R290 at 40°C from NIST Refprop Version 9.0 [27]

		R32	R134a	R1234ze(E)	R245fa	R290
p_S	[bar]	24.783	10.166	7.666	2.505	13.694
ρ_L	[kg m^{-3}]	893.0	1146.7	1111.3	1296.7	467.5
ρ_V	[kg m^{-3}]	73.3	50.1	40.7	14.1	30.2
μ_L	[μPa s]	94.99	161.45	167.00	337.90	82.84
μ_V	[μPa s]	13.83	12.37	12.93	10.76	8.89
λ_L	[W m^{-1} K^{-1}]	0.115	0.075	0.069	0.083	0.087
σ	[mN m^{-1}]	4.47	6.13	6.96	12.12	5.21

First of all, it can be argued that liquid thermal conductivity plays a fundamental role. Inside the circular channel, at G=100 kg m^{-2} s^{-1}, the highest heat transfer coefficients are achieved with R32 which has also the highest liquid thermal conductivity. As expected, R1234ze(E) displays the lowest liquid thermal conductivity and lowest heat transfer coefficient.

As previously stated, for G < 200 kg m^{-2}s^{-1} the effect of mass velocity becomes less relevant. For example, in the case of R32 the heat transfer coefficient-vapour quality curves overlap. It could be interesting to analyze the ratio of heat transfer coefficient at G = 200 to the one at G = 100 kg m^{-2}s^{-1} for the different fluids at a fixed value of vapour quality. For example, at x = 0.5 such heat transfer coefficient ratio inside the 1 mm circular minichannel is about 1.00, 1.24, 1.39, 1.41 and 1.6, respectively for R32, R134a, R1234ze(E), R245fa and R290. The last two fluids, R245fa and R290, which display the largest effect of mass velocity are the fluids with the lowest vapour density and thus highest vapor phase velocity.

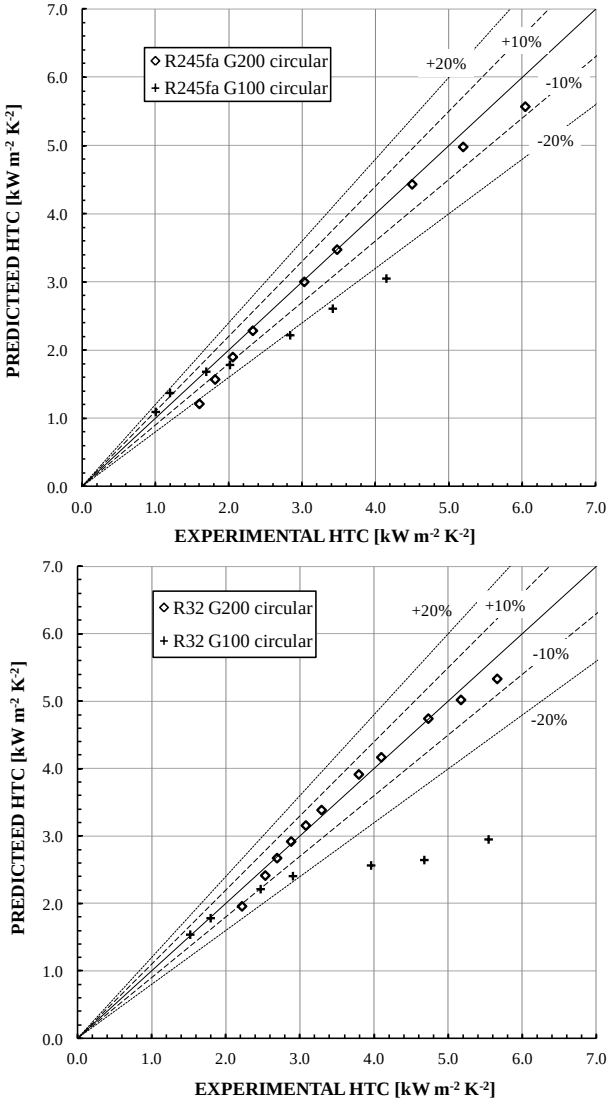

Figure 7 Comparison between measurements and calculated heat transfer coefficients using the model by Cavallini et al. [4]. Top: R245fa. Bottom: R32.

USE OF MACROSCALE PREDICTING PROCEDURE

It was previously demonstrated that at low mass velocity (≤ 200 kg m^{-2}s^{-1}) the microscale effects influence the condensation process. For this reason, the predicting models developed for macroscale condensation, such as Cavallini et al. [4] and Moser et al. [28], cannot be extended to low diameter channels at these conditions.

For example, in Fig. 7 experimental data taken with R245fa and R32 at G = 100 and 200 kg m^{-2} s^{-1} in the round minichannel are compared against predictions by Cavallini et al. [4] model.

It can be seen that when reducing the mass flux the experimental heat transfer coefficients may be underpredicted by this model, to a different extent for different fluids. In other words, models developed for macroscale condensation can still be applied to minichannels but with a lower operating conditions range, avoiding the regions where the role of capillary and gravity forces may introduce differences with microscale data. In this study the dimensionless gas velocity J_V and the two-phase Weber number have been considered as parameters to take into account, respectively, the gravity and surface tension effects. In Fig. 8 the predictions by Cavallini et al. [4] model has been reported for all the experimental data (R134a, R32, R245fa, R1234ze(E), R290) that satisfy the following conditions: $J_V \geq J_{VT}$ and $We \geq We_T$, where the transition numbers J_{VT} and We_T are given as a function of the Martinelli parameter in Eqs 1-2. With such limitations, the model by Cavallini et al. [4] can be applied also at low mass velocities.

$$J_V^T = \left\{ \left[7.5/(4.3X_{tt}^{1.111}+1) \right]^{-3} + C_T^{-3} \right\}^{-1/3};\ C_T = 6 \qquad (1)$$

$$We^T = \left\{ \left[6/(12X_{tt}^{3}+0.1) \right]^{-3} + D_T^{-3} \right\}^{-1/3};\ D_T = 30 \qquad (2)$$

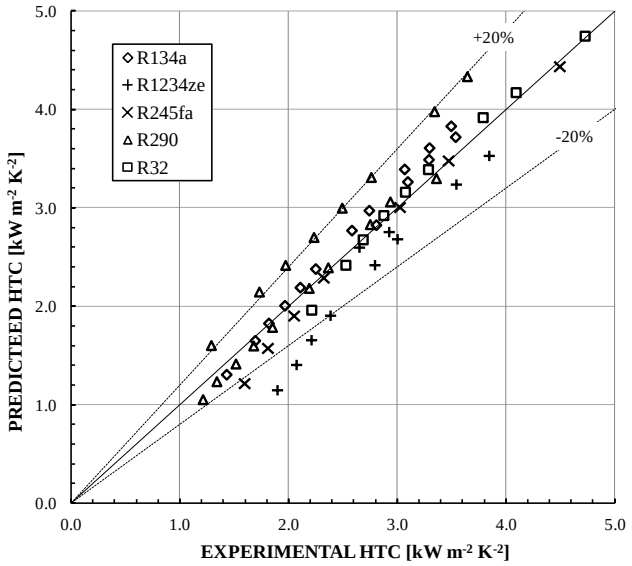

Figure 8 Comparison between measurements and calculated heat transfer coefficients using the model by Cavallini et al. [4] when $J_V \geq J_V^T$ and $We \geq We^T$.

NUMERICAL SIMULATIONS

At low values of Weber number, macroscale models may not provide accurate predictions. The simultaneous effect of vapour velocity, gravity and surface tension makes the condensing process very difficult to be predicted. An alternative path consists of numerical simulation of the vapour-liquid flow, tracking the interface during the heat transfer process. In this section, three-dimensional simulations of condensation of different refrigerants in a horizontal 1 mm i.d. minichannel with circular and square cross section are reported. The simulations have been performed under steady-state conditions. This setting does not allow to simulate the intermittent flow, i.e. slug/plug flow, the presence of waves on vapour-liquid interface and the entrainment of liquid droplets by interface shear stresses to the vapor core. A uniform interface temperature equal to the saturation one and a uniform wall temperature have been fixed as boundary conditions. The volume of fluid method is used to track the vapour-liquid interface, and the effects of interfacial shear stress, surface tension and gravity have been taken into account.

The circular minichannel mesh is formed of around $1.15 \cdot 10^6$ hexahedrons cells and the symmetry conditions for both cross section shapes have been applied. In order to fully resolve the liquid film region, the radial thickness of the cells in the near-wall region is around 0.8 μm, while the mesh is much coarser in the core region due to computation cost reasons; and 450 nodes are used for the axial discretization. In the case of square minichannel, the domain is discretized into $3.88 \cdot 10^6$ hexahedrons cells; the radial thickness of the cells in the near-wall region is around 1 μm, while the mesh is much coarser in the core region; 385 nodes are used for axial discretization.

In the present work, two different computational approaches have been considered. The first approach (referred to as "laminar liquid film") is the most common in microscale condensation and corresponds to the assumption that the flow is laminar in the liquid phase and turbulent in the vapour one. In this approach the standard low-Re formulation by Wilcox [29] is applied for the vapour phase, while a null turbulent viscosity is set in the liquid phase and blended between the two values at the interface; in this way, laminar flow is imposed inside the liquid phase and the turbulence production is suppressed. In the second approach (referred to as "SST k-ω approach" in the paper), instead, a low Reynolds form of a turbulence model, as reported by Menter [30] has been used through the whole computational domain.

A detail description about the volume of fluid (VOF) method and the turbulence issue is reported in Da Riva et al. [31].

Effect of the cross section shape

As demonstrated numerically by Bortolin et al. [12] (Fig. 9), at high mass flux there is almost no effect of the channel cross section shape on the heat transfer coefficient. At such conditions, condensation is controlled by vapor shear stress, and this can be understood considering the dominating role of the mass flux. Da Riva et al. [31] pointed out that such dependence, observed in almost all experimental works, can be predicted by numerical simulations only if the laminar film hypothesis is relaxed and some turbulence is accounted for in the liquid film. In these conditions, the shape of the vapor-liquid interface, which is in any case affected by surface tension, does not have a real influence on the heat transfer coefficient because the governing parameter is the effective liquid thermal conductivity induced by turbulence.

Since surface tension effects at high mass velocity are masked by vapor shear stress, in the following numerical simulations will be presented only at $G \leq 200$ kg m^{-2} s^{-1} and compared against experimental data. In Table 2, all the simulations performed are summarized.

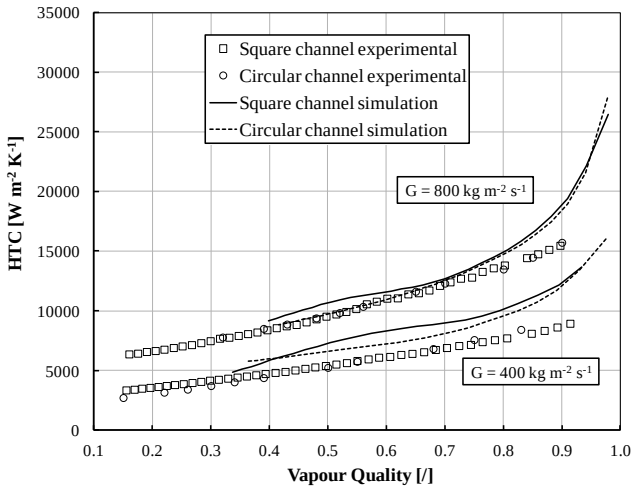

Figure 9 Cross-sectional average heat transfer coefficient as a function of vapour quality inside 1 mm diameter square and circular minichannel at G = 400 kg m^{-2}s^{-1} and 800 kg m^{-2}s^{-1} (Bortolin et al. [12]).

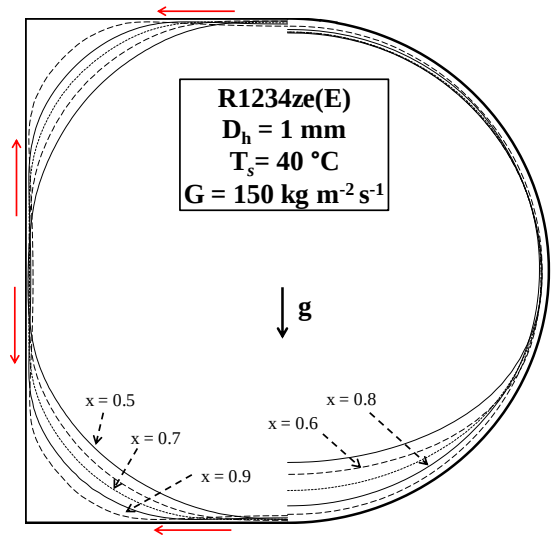

Figure 10 Liquid-vapour interface tracked by means of VOF numerical simulations in circular and square minichannel at varying vapour qualities during condensation, at G=150 kg m^{-2} s^{-1} and 40°C saturation temperature.

In Fig. 10, the liquid-vapour interface is tracked by VOF simulations in circular and square 1 mm i.d. minichannel during R1234ze(E) condensation, at G = 150 kg m^{-2}s^{-1}. As can be seen, the distribution of liquid film in the square and in the circular channel is completely different. In fact, in the square channel, surface tension pulls the liquid towards the corners and a thin liquid film forms at the centre of each flat side. No stratification is observed, even at vapor quality x = 0.5. Instead, in the case of the circular channel, the gravity force is found to promote liquid stratification also at such low channel dimension. Since the surface tension and the gravity forces drive the liquid film distribution, the effects of the cross section shape and of minichannel inclination become important for the evaluation of the condensation heat transfer coefficient.

Table 2 Cases of numerical simulations

Fluid	G [kg m^{-2} s^{-1}]	Section shape	Turbulence approach Liquid film	Length [mm]	Outlet quality
R134a	65	circular	Laminar	35	0.57
R134a	100	circular	Laminar	75	0.44
R134a	200	circular	Laminar	120	0.50
R32	100	circular	Laminar	50	0.58
R32	200	circular	Laminar	135	0.45
R1234ze(E)	150	circular	Laminar	120	0.39
R245fa	100	circular	Laminar	100	0.30
R245fa	100	circular	SST k-ω	45	0.47
R245fa	200	circular	Laminar	180	0.35
R245fa	200	circular	SST k-ω	85	0.34
R290	100	circular	Laminar	150	0.41
R290	200	circular	Laminar	270	0.43
R290	200	circular	SST k-ω	120	0.37
R134a	65	square	Laminar	35	0.53
R134a	100	square	Laminar	50	0.50
R134a	200	square	Laminar	90	0.53
R32	100	square	Laminar	65	0.46
R32	200	square	Laminar	120	0.44
R1234ze(E)	150	square	Laminar	90	0.42

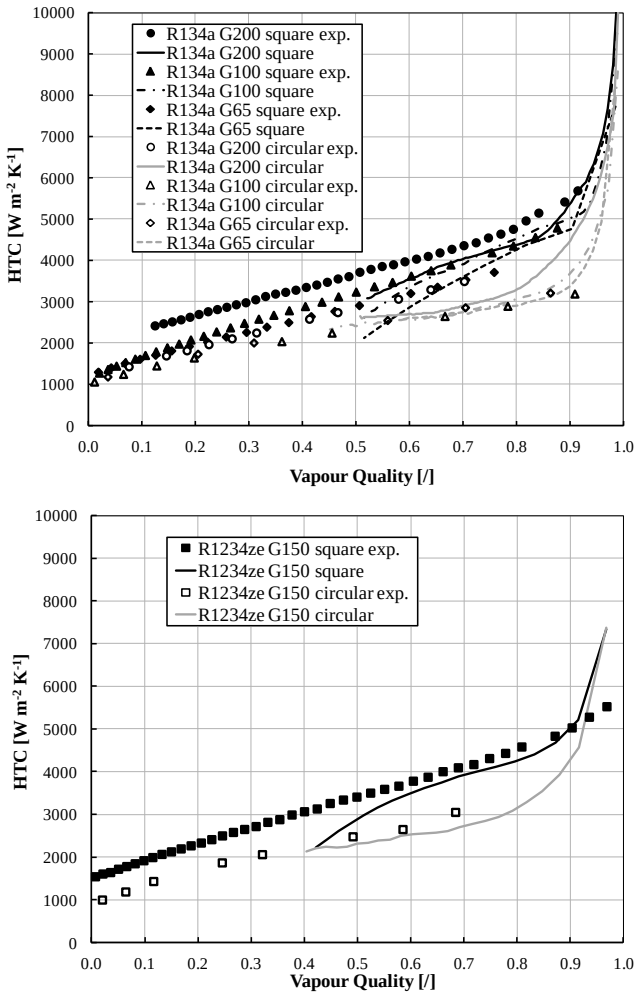

Figure 11 Experimental and calculated condensation heat transfer coefficients using VOF simulations. Top: R134a. Bottom: R1234ze(E).

In Fig. 11 experimental and calculated heat transfer coefficients assuming laminar liquid film are shown in the case of R134a and R1234ze. In the case of R134a, a good agreement between simulations and experimental data is found. It should be noticed that for $x > 0.6$ the enhancement of the heat transfer coefficient in the square channel with respect to the circular one is reproduced by numerical simulations.

As can be seen in Fig. 11, for vapour quality below 0.5, the heat transfer coefficient inside the circular minichannel becomes higher than that inside the square minichannel. This result is found only in numerical simulations and it is also predicted by the Wang and Rose [19] theoretical model. On the contrary, experimental data by the present authors (in agreement with data by Liu et al. [10]) show a higher heat transfer coefficient for the square also at low values of vapor quality. With the hypothesis of annular flow, it is shown as surface tension prevents liquid stratification in the square channel (Fig. 12). In the case of the circular channel, liquid stratification causes a thinning of the condensate thickness in the upper part of the channel, where almost all the heat flow rate is rejected. Therefore, at low vapor qualities, from the heat transfer point of view, it is preferable to have a part of the wall with reduced liquid film thickness than a uniformly distributed liquid film. From visualization studies (Coleman and Garimella [32]) a transition region between annular and plug/slug flow is expected at these conditions. This could explain the discrepancy found between numerical simulations and experiments at low quality ($x < 0.5$).

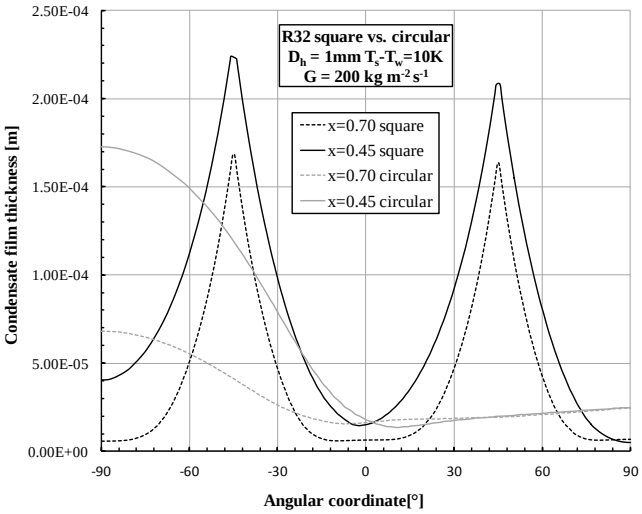

Figure 12 Condensate film thickness as a function of the angular coordinate at G= 200 kg m^{-2} s^{-1} during R32 condensation at two values of vapour quality.

Effect of the refrigerant properties

Experimental and calculated heat transfer coefficients for R134a, R1234ze(E), R32, R245fa and R290 with mass fluxes between 65 and 200 kg m^{-2} s^{-1} inside both circular and square minichannel are reported in Figs. 11, 13, 14. In Table 3 the average deviation e_R between experimental results and numerical simulations is reported for all the simulated cases. At G = 100-150 kg m^{-2} s^{-1} the condensation heat transfer coefficient of R290, R134a and R1234ze(E) are predicted by the laminar liquid film approach with deviations below 11%.

Let's now consider the case of R134a: at G = 200 kg m^{-2} s^{-1} the laminar liquid film approach underpredicts experimental results with an average deviation e_R = -16%, whereas the turbulent film approach (SST k-ω), as reported in Da Riva et al. [31], overpredicts by around 50% the experimental data. A similar behavior has been found for R1234ze(E) since these two refrigerants have similar properties. This poses a question mark on the turbulence transition in the liquid film at the present operating conditions.

Table 3 Comparison between experimental and calculated cross section average heat transfer coefficients

Refrigerant	G [kg m^{-2} s^{-1}]	Section shape	Turbulence approach Liquid film	e_R [%]	σ_N [%]
R134a	65	circular	Laminar	-3.6	1.6
R134a	100	circular	Laminar	6.4	7.7
R134a	200	circular	Laminar	-15.7	2.6
R32	100	circular	Laminar	-20.0	5.5
R32	200	circular	Laminar	-9.5	6.3
R1234ze(E)	150	circular	Laminar	-9.4	4.0
R245fa	100	circular	Laminar	-24.1	4.4
R245fa	100	circular	SST k-ω	16.0	3.9
R245fa	200	circular	Laminar	-42.7	7.5
R245fa	200	circular	SST k-ω	24.2	8.1
R290	100	circular	Laminar	-11.5	6.7
R290	200	circular	Laminar	-41.8	1.5
R290	200	circular	SST k-ω	51.3	1.6
R134a	65	square	Laminar	-7.3	10.2
R134a	100	square	Laminar	-4.8	9.5
R134a	200	square	Laminar	-9.2	4.4
R32	100	square	Laminar	-8.8	14.3
R32	200	square	Laminar	-11.1	14.6
R1234ze(E)	150	square	Laminar	-8.0	8.0

At G=200 kg m^{-2} s^{-1} the laminar liquid film assumption works well only in the case of refrigerant R32 (Fig. 13). It should be noticed that R32 is the fluid that displays the highest vapor density and thus the lowest vapor velocity.

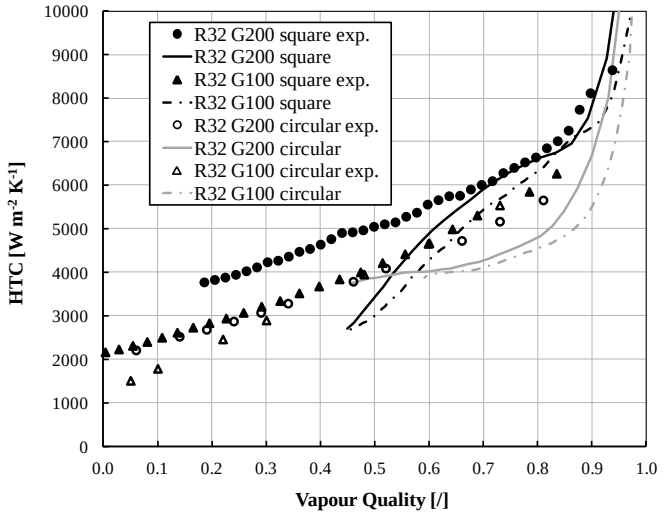

Figure 13 Experimental and calculated heat transfer coefficients by means of VOF simulations for R32.

Fig. 14 displays the results for R245fa: it is the only fluid among those investigated here for which the heat transfer coefficient predictions by the SST *k-ω* approach are better than those obtained by the laminar liquid film approach at both mass fluxes (100-200 kg $m^{-2}s^{-1}$). Furthermore, it was found experimentally that with this fluid the effect of mass velocity on the heat transfer coefficient is still important also at such low values of *G*. On the contrary, for R32, R1234ze(E), and R134a, the experimental heat transfer coefficients at 100 and 200 kg m^{-2} s^{-1} almost overlaps.

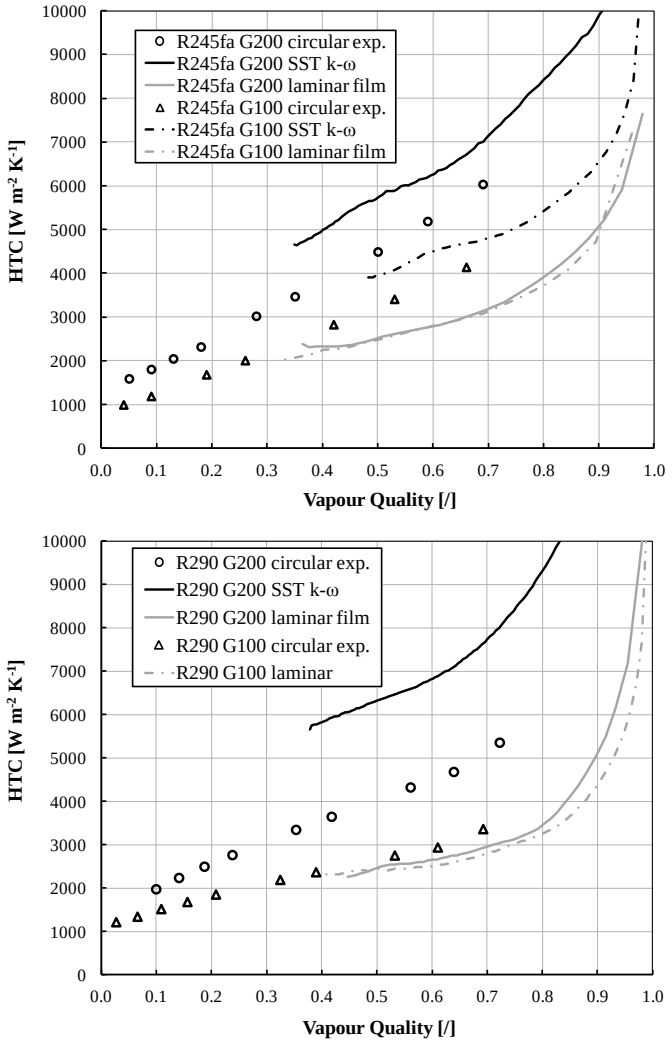

Figure 14 Experimental and calculated heat transfer coefficients by means of VOF simulations. Top: results for R245fa. Bottom: results for R290.

Since the present issue regards the possible occurrence of some turbulence in the liquid film, it may be interesting to look at available criteria to determine whether the laminar film assumption should be relaxed. Cioncolini and Thome [25] reported an algebraic turbulence modeling in adiabatic and evaporating annular two-phase flow, focusing in particular on momentum and heat transfer through the annular liquid film. With assumption of shear-driven annular liquid films as fluid-bounded flows, this turbulence model provides both velocity and temperature profiles through the liquid films and relates both turbulent eddy diffusivities v_t^+ and α_t^+ with the length scale characteristic, which should capture the size of the turbulent eddies in shear-driven annular films. In this algebraic model the length scale that is assumed to characterize shear-driven annular films is the dimensionless average liquid film thickness t^+. For low values of t^+ both turbulent eddy diffusivities are predicted to be null. This means that the turbulence is not presence in the liquid film, so it is laminar. In this section, the algebraic model has been applied and the average film thickness *t* and the wall shear stress τ_W have been calculated as cross-sectional averages from the numerical simulations and the liquid properties have been evaluated at the wall temperature and saturation pressure, as listed in Table 1.

As depicted in Fig. 15, it is worth noting that, for a given mass velocity and vapor quality, R245fa has the lowest dimensionless film thickness, suggesting a transition to turbulent flow at higher mass velocities than the ones considered in the present study. This could be due to high liquid dynamic viscosity of R245fa, since it is a key-parameter influencing the dimensionless liquid film thickness. However, this criterion does not agree with the assumptions of some turbulence in the liquid film at G = 100 kg $m^{-2}s^{-1}$ during R245fa condensation that arises from the previous comparison between experimental data and numerical simulations. From these results, it can be concluded that R245fa displays a strong effect of mass flux on the heat transfer coefficient between 100 and 200 kg $m^{-2}s^{-1}$, with high *We* number, but at such low mass velocities the value of dimensionless liquid film thickness is too low to permit some turbulence occur in the liquid film. Therefore, the present simulations do not seem to reproduce the physical phenomena occurring in the two-phase flow and the reason may be that such phenomena are typically unsteady, with presence of waves at the vapour-liquid interface that would require an unsteady approach in the numerical simulations.

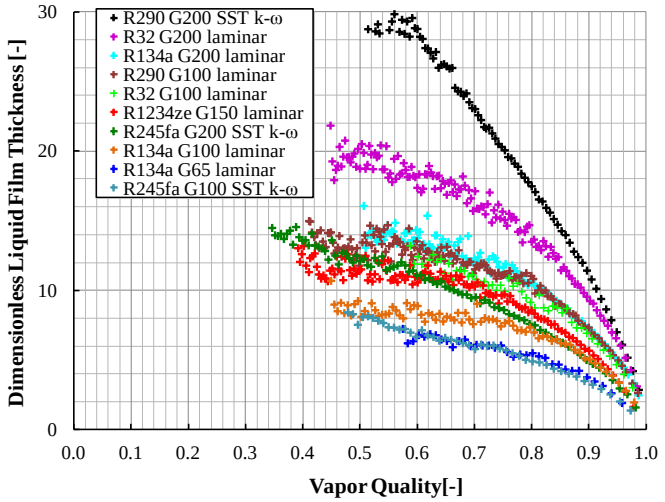

Figure 15 Dimensionless liquid film thickness for R134a, R1234ze(E), R32, R290 and R245fa at different mass velocities inside a 1 mm diameter circular cross section minichannel.

CONCLUSIONS

Experimental data and three dimensional numerical simulations of R134a, R32, R245fa, R290 and R1234ze(E) condensation inside horizontal 1 mm diameter minichannels with circular and square cross section shapes have been reported. The following conclusions can be drawn:

- At high mass velocities (e.g. $G \geq 400$ kg $m^{-2}s^{-1}$) condensation is dominated by shear stress, with no effects of channel shape and inclination on the heat transfer coefficient. Furthermore, correlations originally developed for macroscale condensation can be successfully extended to lower diameters.
- At low value of mass velocity (e.g. $G \leq 200$ kg m^{-2} s^{-1}), surface tension can play an important role and microscale effects appear. In particular, for vapor quality $x > 0.5$ both numerical simulations and experimental results show a clear enhancement of the heat transfer coefficient in the square channel with respect to the circular one. Such enhancement, is due to the surface tension that, in the square channel, pulls the liquid towards the corners leading to a low film thickness on the flat sides of the channel.
- Despite the small channel diameter, in the case of circular tube, at low mass velocity, some liquid stratification due to gravity is however expected.
- The Cavallini et al. [4] model, developed for conventional channels, may underpredict some experimental data when reducing the mass velocity. A criterion depending on the Weber number is given to establish the applicability region of the macroscale condensation model. Still, the problem of predicting the heat transfer coefficients in the region of low *We* number is an open issue.
- A reasonably good agreement between numerical simulations and experimental data was found. It may be interesting noting that at $G = 100$ kg m^{-2} s^{-1} the laminar liquid film approach works well for all the refrigerants except for R245fa.
- From the comparison between experimental data and numerical simulations, it seems that for each fluid there may be a range of operating conditions which are well predicted assuming a range of laminar liquid film and a range of transient and turbulent liquid flow.
- The R245fa condensation data at $G = 100$ kg $m^{-2}s^{-1}$ are estimated using the SST k-ω approach in liquid film with better agreement than using the laminar film approach. The physical reason is probably related to the vapor velocity which is higher than for other fluids and may have some effect at the interface between liquid and vapor.
- Further experimental investigation is needed at low mass velocities. In particular, there is need for numerical simulations in the intermittent regime and in the wavy annular flow regime.

REFERENCES

[1] Kew P.A., and Reay D.A., Compact/micro-heat exchangers - Their role in heat pumping equipment, *Applied Thermal Engineering*, Vol. 31, 2011, pp. 594-601.

[2] Nema G., Garimella S., and Fronk B.M., Flow regime transitions during condensation in microchannels, *Int. J. Refrigeration*, Vol. 40, 2014, pp. 227-240.

[3] Coleman J.W., and Garimella S., Two-phase flow regimes in round, square and rectangular tubes during condensation of refrigerant R134a, Int. J. Refrigeration, Vol. 26, 2003, pp. 117-128.

[4] Cavallini A., Del Col D., Doretti L., Matkovic M., Rossetto L., Zilio C., and Censi G., Condensation in horizontal smooth tubes: A new heat transfer model for heat exchanger design, *Heat Transfer Engineering*, Vol. 27, 2006, pp. 31-38.

[5] Cavallini A., Bortolin S., Del Col D., Matkovic M., and Rossetto L., Condensation heat transfer and pressure losses of high- and low-pressure refrigerants flowing in a single circular minichannel, *Heat Transfer Engineering*, Vol. 32, 2011, pp. 90-98.

[6] Del Col D., Bortolin S., Cavallini A., and Matkovic M., Effect of cross sectional shape during condensation in a single square minichannel, *Int. J. Heat Mass Transfer*, Vol. 54, 2011, pp. 3909-3920.

[7] Del Col D., Bortolato M., Azzolin M., and Bortolin S., Condensation heat transfer and two-phase frictional pressure drop in a single minichannel with R1234ze(E) and other refrigerants, *Int. J. Refrig.*, Vol. 50, 201, pp. 87-103.

[8] Bandhauer T. M., Agarwal A., and Garimella, S., Measurement and modeling of condensation heat transfer coefficients in circular microchannels, *Trans. ASME Journal of Heat Transfer*, Vol. 128(10), 2006, pp. 1050–1059.

[9] Matkovic M., Cavallini A., Del Col D., and Rossetto L., Experimental study on condensation heat transfer inside a single circular minichannel, *Int. J. Heat Mass Transfer.*, Vol. 52, 2009 pp. 2311-2323.

[10] Liu N., Li J.M., Sun J., Wang H.S., Heat transfer and pressure drop during condensation of R152a in circular and square microchannels, *Exp. Therm. Fluid Sci.*, Vol. 47, 2013, pp. 60-67.

[11] Sakamatapan K., Kaew-On J., Dalkilic A. S., Mahian O., and Wongwises S., Condensation heat transfer characteristics of R-134a flowing inside the multiport minichannels, *International Journal of Heat and Mass Transfer*, Vol. 64, 2013, pp. 976-985.

[12] Bortolin S., Da Riva E., and Del Col D., Condensation in a square minichannel: Application of the VOF method, *Heat Transfer Engineering*, Vol.35, 2014, pp. 193-203.

[13] Del Col D., Bortolato M., Azzolin M., and Bortolin S., Effect of inclination during condensation inside a square cross section minichannel, *Int. J. Heat Mass Transfer*, Vol. 78, 2014, pp. 760-777.

[14] Da Riva E., and Del Col D., Effect of gravity during condensation of R134a in a circular minichannel, *Microgravity Science and Technology*, Vol. 23(Suppl. 1), 2011, pp. 87–97.

[15] Marchuk I., Lyulin Y., and Kabov O., Theoretical and experimental study of convective condensation inside a circular tube, *Interfacial Phenomena and Heat Transfer*, Vol. 1(2), 2013, pp. 153-171.

[16] Garimella S., Fronk B.M., Milkie J.A., and Keinath B., Versatile models for condensation of fluids with widely varying properties from the micro to macroscale, *Proceedings of the 15th International Heat Transfer Conf., IHTC-15*, 2014, 10516.

[17] Wang H. S., and Rose J. W., A theory of film condensation in horizontal non-circular section microchannels, *Trans. ASME Journal of Heat Transfer*, Vol. 127(10), 2005, pp. 1096–1105.

[18] Wang H. S., and Rose J. W., Film condensation in horizontal circular-section microchannels, *International Journal of Engineering Systems Modelling and Simulation*, Vol. 1, 2009, pp. 115-121.

[19] Wang H. S., and Rose, J. W., Theory of heat transfer during condensation in microchannels, *International Journal of Heat and Mass Transfer*, Vol. 54, 2011, pp. 2525-2534.

[20] Nebuloni S., and Thome J. R., Numerical modeling of laminar annular film condensation for different channel shapes, *Int. J. Heat Mass Transfer*, Vol. 53, 2010, pp. 2615–2627.
[21] Ganapathy H., Shooshtari A., Choo K., Dessiatoun S., Alshehhi M., and Ohadi M., Volume of fluid-based numerical modeling of condensation heat transfer and fluid flow characteristics in microchannels, *International Journal of Heat and Mass Transfer*, Vol. 65, 2013, pp. 62-72.
[22] Shah M. M., An improved and extended general correlation for heat transfer during condensation in plain tubes, *HVAC&R Research*, Vol. 15(5), 2009, pp. 889-913.
[23] El Mghari H., Asbik M., Louahlia-Gualous H., and Voicu I., Condensation heat transfer enhancement in a horizontal non-circular microchannel, *Applied Thermal Engineering*, Vol. 64, 2014, pp. 358-370.
[24] Antonsen N., and Thome J.R., Numerical simulation of condensing and evaporating annular flows in microchannels with laminar and turbulent liquid films, *Proceedings of the 15th International Heat Transfer Conf., IHTC-15*, 2014, 9798.
[25] Cioncolini A., and Thome J.R., Algebraic turbulence modeling in adiabatic and evaporating annular two-phase flow, *Int. J. Heat Fluid Flow*, Vol. 32, 2011, pp. 805-817.
[26] Del Col D., Bortolato M., and Bortolin S., Comprehensive experimental investigation of two-phase heat transfer and pressure drop with propane in a minichannel, *Int. J. Refrigeration*, Vol. 47, 2014, pp. 66-84.
[27] Lemmon E.W., Huber M.L., and McLinden, M.O., 2010. NIST Standard Reference Database 23: Reference Fluid Thermodynamic and Transport Properties-REFPROP, Version 9.0. National Institute of Standards and Technology, Standard Reference Data Program, Gaithersburg.
[28] Moser K.W., Webb R.L., and Na B., A new equivalent Reynolds number model for condensation in smooth tubes, *Journal of Heat Transfer*, Vol. 120, 1998, pp. 410-417.
[29] Wilcox D.C., Turbulence Modeling for CFD, second ed., DCW Industries, Inc., La Cañada,CA, USA, 1998.
[30] Menter F.R., Two-equation eddy-viscosity turbulence models for engineering applications, *AIAA J*., Vol. 32, 1994 pp. 1598-1605.
[31] Da Riva E., Del Col D., Garimella S.V., Cavallini A., The importance of turbulence during condensation in a horizontal circular minichannel, *Int. J. Heat Mass Transfer* Vol. 55, 2012, pp. 3470-3481.
[32] Coleman J.W., and Garimella S., Two-phase flow regime transitions in microchannel tubes: the effect of hydraulic diameter, *ASME HTD*, Vol. 366-4, (2000) pp. 71–83.